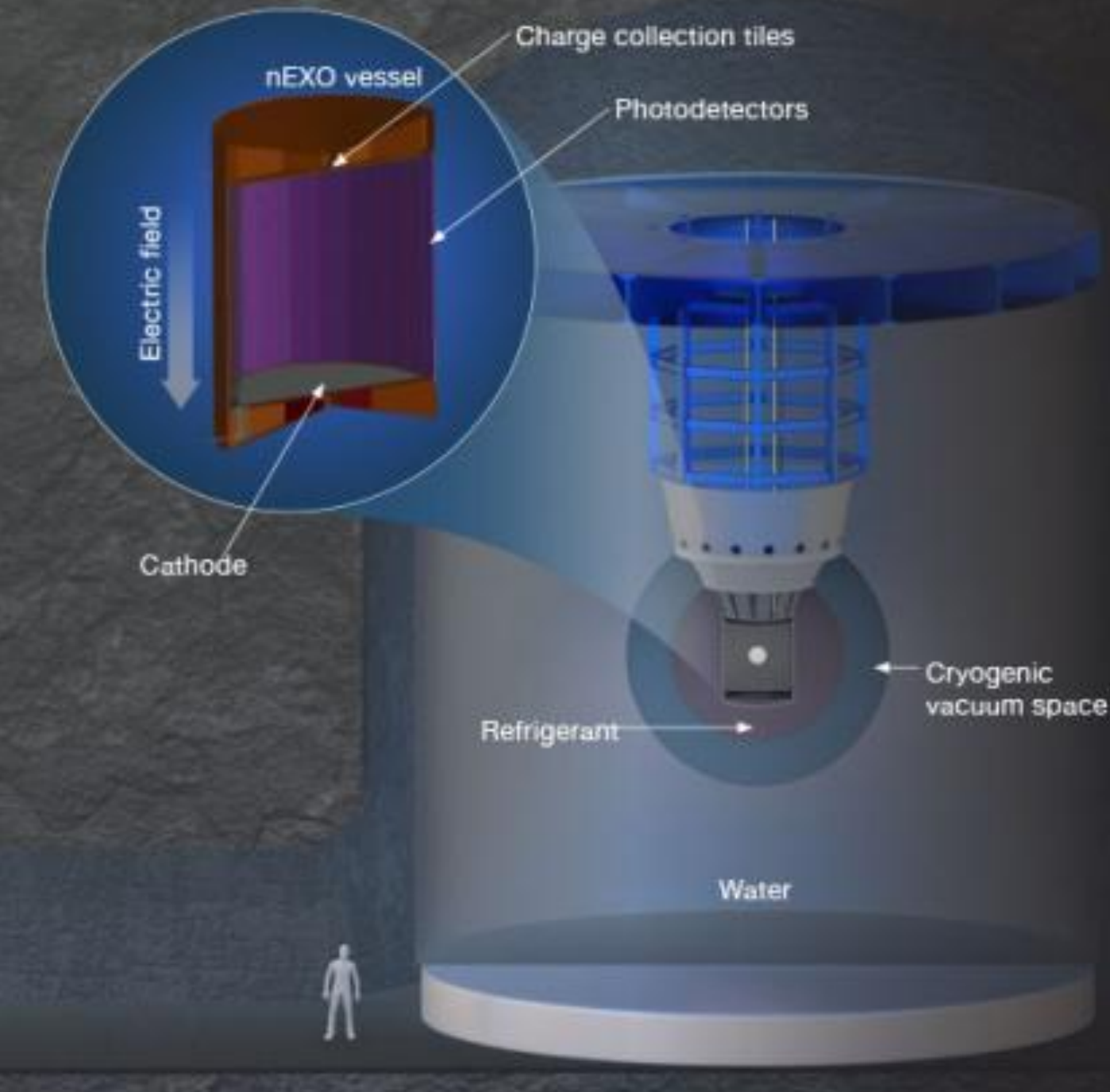




# 实验进展

李高嵩  
中科院高能所

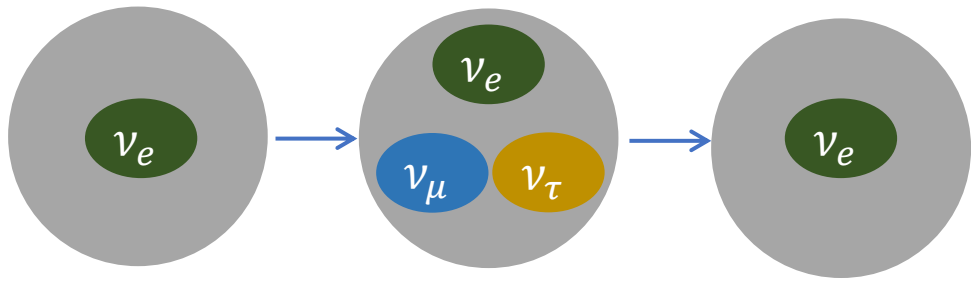
$0\nu\beta\beta$ 研讨会  
中山大学，珠海  
2021年5月22日



# Outline

- $0\nu\beta\beta$  decay
- Liquid Xenon TPC technology
- EXO-200, prototype demonstration of nEXO
- nEXO design
- R&D and IHEP efforts
- Conclusion

# Neutrino oscillation



Massive  
neutrinos!

$$U_{PMNS} = \begin{pmatrix} 1 & 0 & 0 \\ 0 & \cos\theta_{23} & \sin\theta_{23} \\ 0 & -\sin\theta_{23} & \cos\theta_{23} \end{pmatrix} \begin{pmatrix} \cos\theta_{13} & 0 & e^{-i\delta} \sin\theta_{13} \\ 0 & 1 & 0 \\ -e^{i\delta} \sin\theta_{13} & 0 & \cos\theta_{13} \end{pmatrix} \begin{pmatrix} \cos\theta_{12} & \sin\theta_{12} & 0 \\ -\sin\theta_{12} & \cos\theta_{12} & 0 \\ 0 & 0 & 1 \end{pmatrix}$$

$$\theta_{23} \approx 45^\circ$$

Accelerator + Atmospheric

$$\theta_{13} \approx 10^\circ$$

Reactor + Accelerator

$$\theta_{12} \approx 35^\circ$$

Solar + Reactor

The Nobel Prize in Physics  
2015

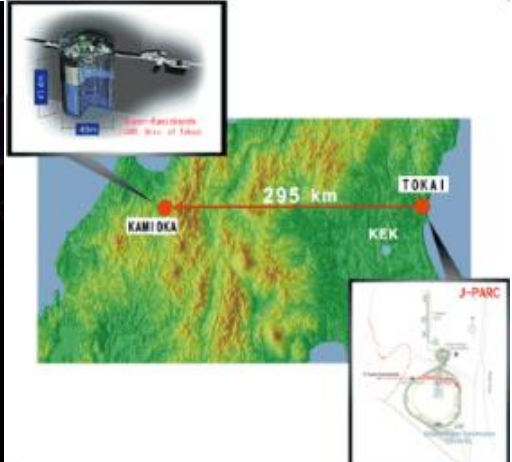
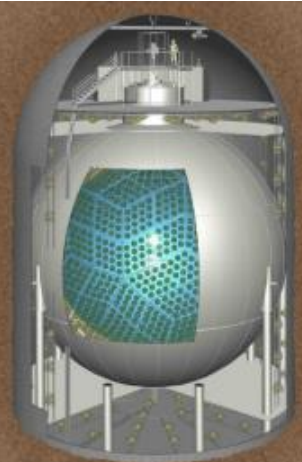
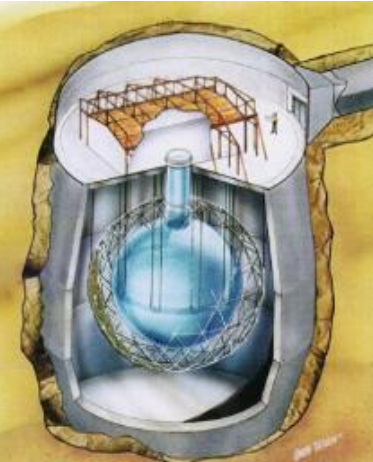
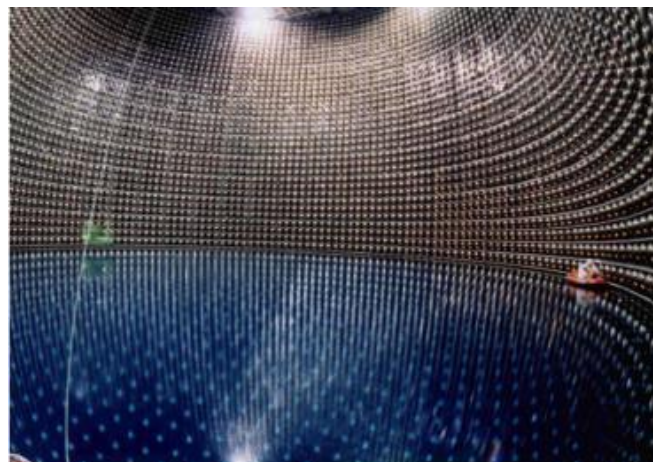


Photo: A. Mahmoud  
Takaaki Kajita  
Prize share: 1/2



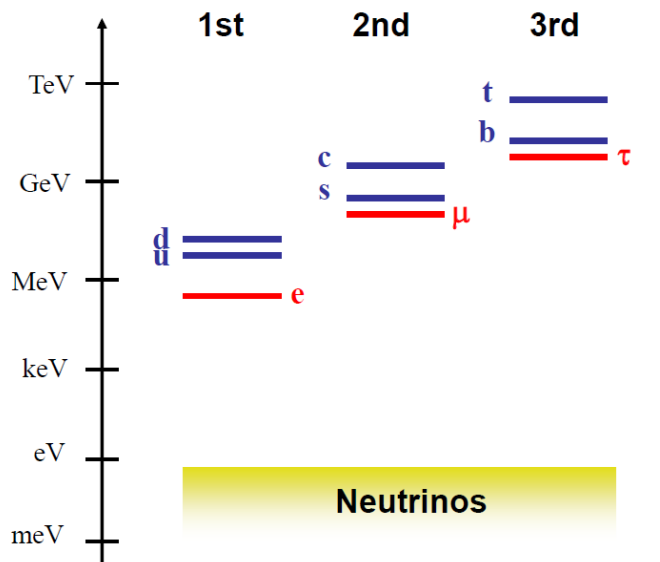
Photo: A. Mahmoud  
Arthur B. McDonald  
Prize share: 1/2

The Nobel Prize in Physics 2015 was awarded jointly to Takaaki Kajita and Arthur B. McDonald "for the discovery of neutrino oscillations, which shows that neutrinos have mass"

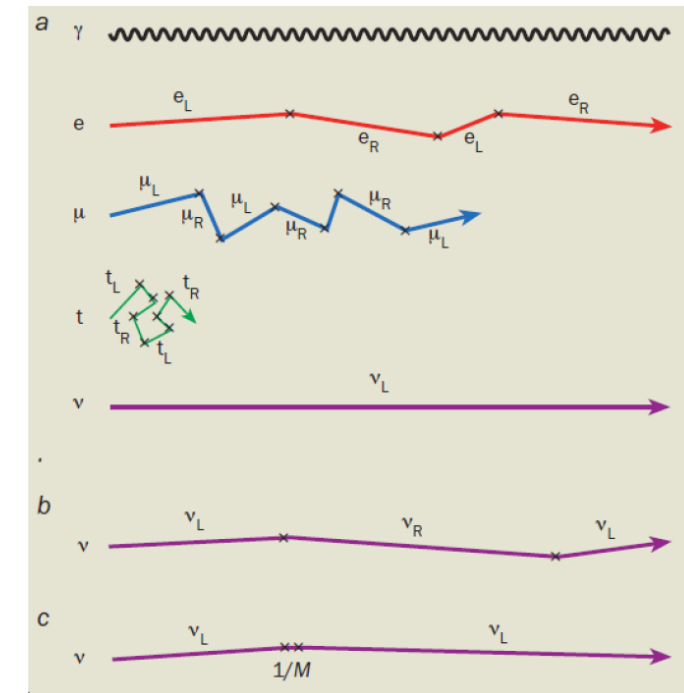


# Neutrino mass generation mechanism

- Neutrino oscillation experiments demonstrate neutrinos have non-zero mass
- Neutrino mass is significantly smaller than other fermions
- **Majorana nature** of neutrinos allows a natural way to explain the small neutrino mass by see-saw mechanism

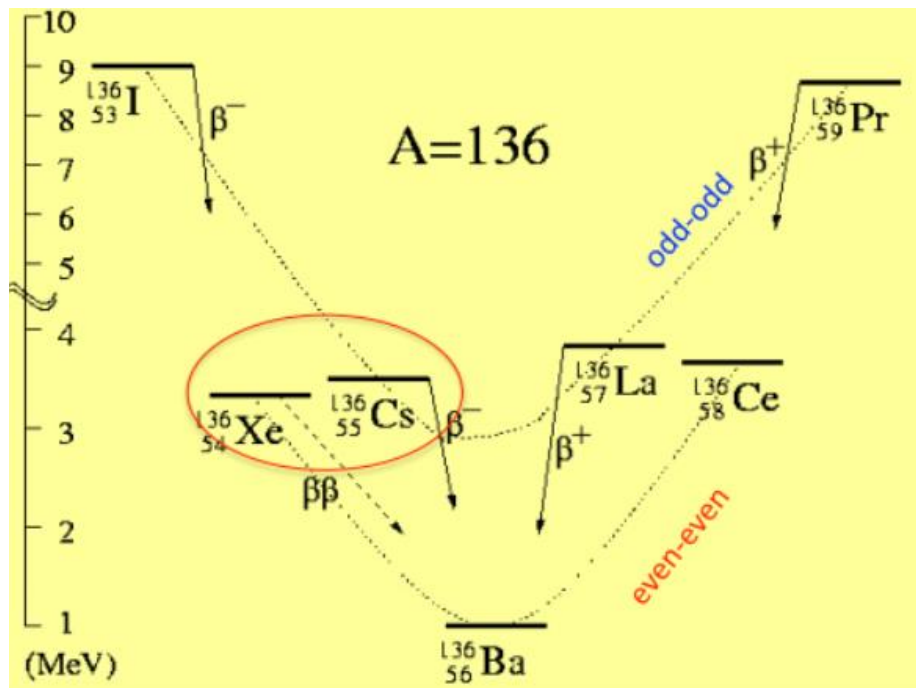


The search for  $0\nu\beta\beta$  is the most sensitive probe of Majorana nature of neutrinos.



# Double beta decay

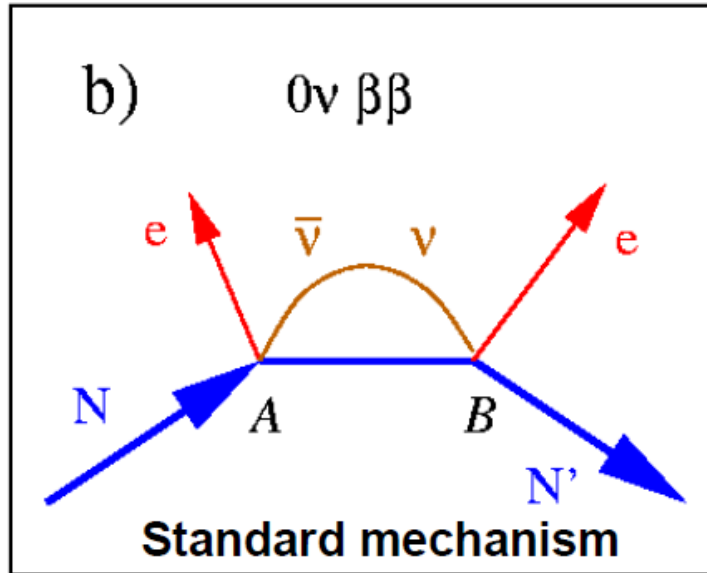
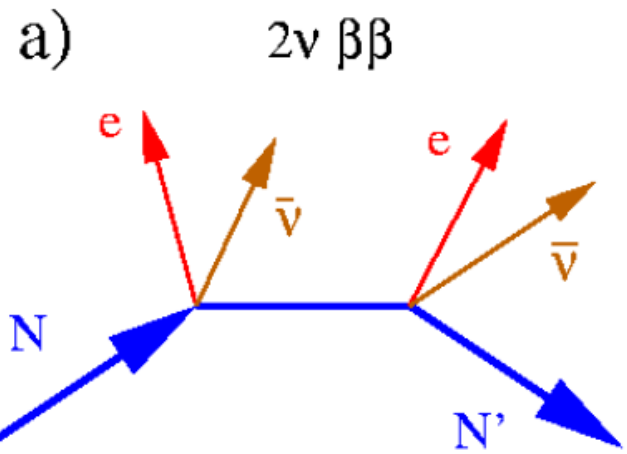
- Double beta decay is a second order process
- Only observable if first order beta decay is energetically forbidden



Candidate with Q>2 MeV

Candidate	Q (MeV)	Abund. (%)
$^{48}\text{Ca} \rightarrow ^{48}\text{Ti}$	4.271	0.187
$^{76}\text{Ge} \rightarrow ^{76}\text{Se}$	2.040	7.8
$^{82}\text{Se} \rightarrow ^{82}\text{Kr}$	2.995	9.2
$^{96}\text{Zr} \rightarrow ^{96}\text{Mo}$	3.350	2.8
$^{100}\text{Mo} \rightarrow ^{100}\text{Ru}$	3.034	9.6
$^{110}\text{Pd} \rightarrow ^{110}\text{Cd}$	2.013	11.8
$^{116}\text{Cd} \rightarrow ^{116}\text{Sn}$	2.802	7.5
$^{124}\text{Sn} \rightarrow ^{124}\text{Te}$	2.228	5.64
$^{130}\text{Te} \rightarrow ^{130}\text{Xe}$	2.533	34.5
$^{136}\text{Xe} \rightarrow ^{136}\text{Ba}$	2.458	8.9
$^{150}\text{Nd} \rightarrow ^{150}\text{Sm}$	3.367	5.6

# Neutrinoless double beta decay ( $0\nu\beta\beta$ )

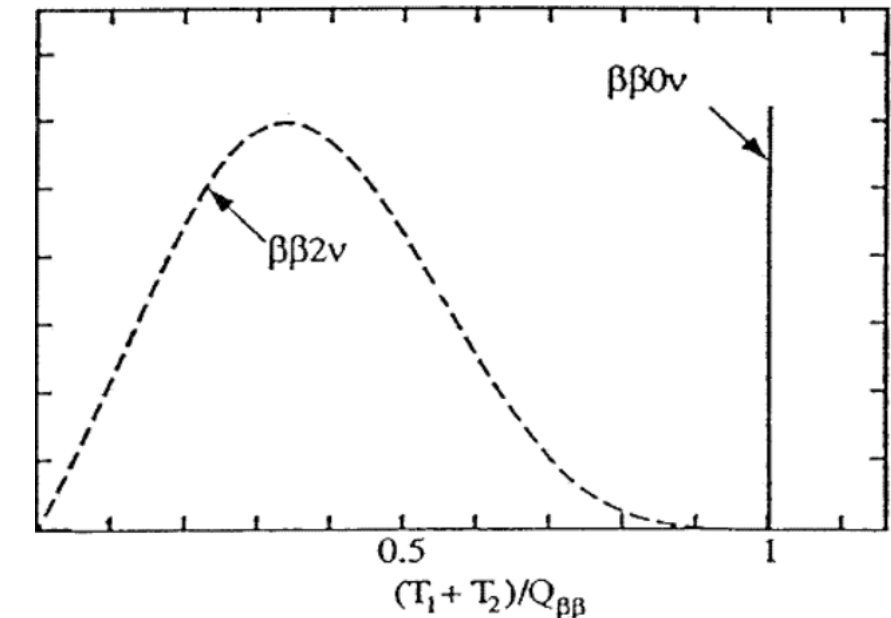


$2\nu\beta\beta$  decay

- Conventional process

$0\nu\beta\beta$  has huge physics implications:

- **Majorana neutrino**
- **Lepton number violation**
- **Absolute neutrino mass scale**

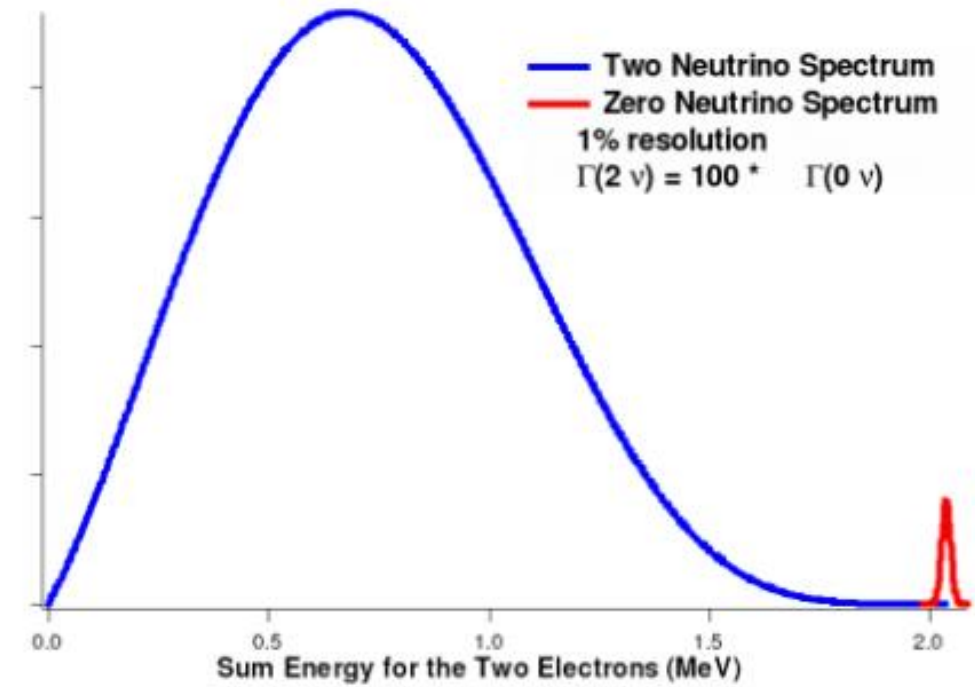


- $2\nu$  VS  $0\nu$  spectrum: continuum vs peak
- Good energy resolution required to separate  $0\nu$  from  $2\nu$

# Experimental sensitivity

$$t_{1/2} \sim \sqrt{\frac{MT}{B \times \Delta E}}$$

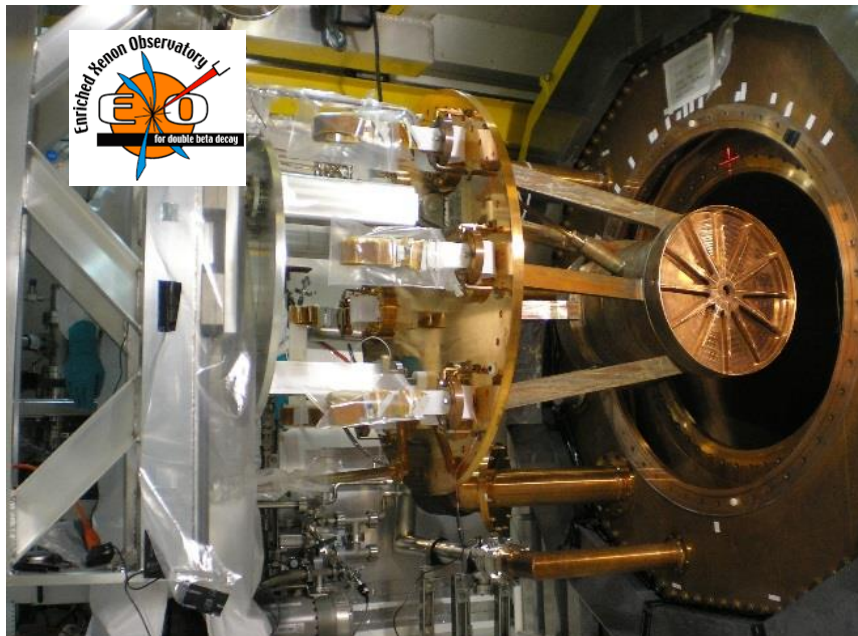
- large detector mass
- low background level
  - low radioactivity detector
  - powerful background rejection
- high energy resolution



# Searching for $0\nu\beta\beta$ in $^{136}\text{Xe}$ , a phased approach

## EXO-200:

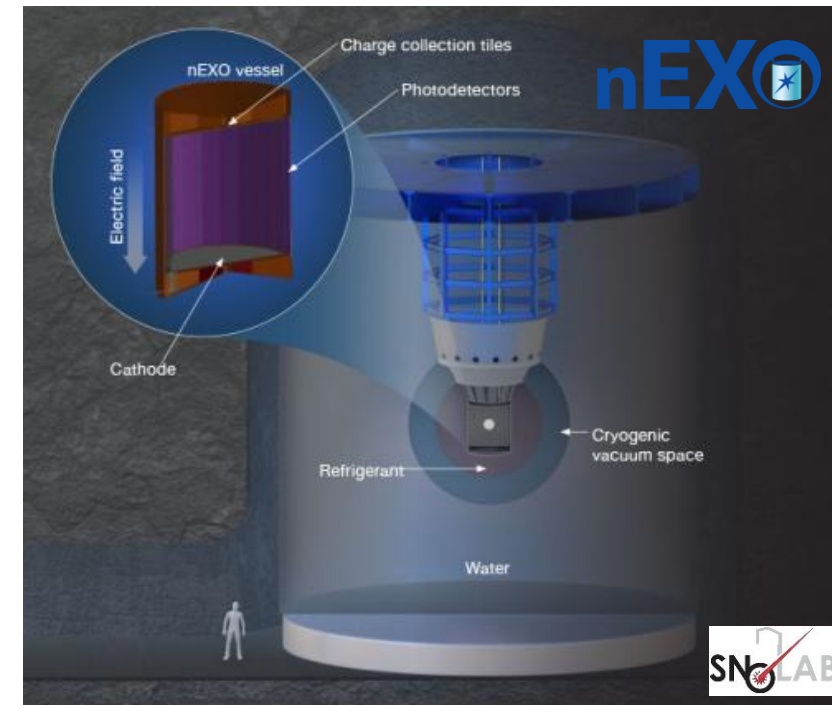
- EXO-200 first 100-kg class  $\beta\beta$  experiment
- Discovery of  $2\nu\beta\beta$  in Xe-136
- 200 kg liquid-Xe TPC with ~80% Xe-136
- Located at the WIPP mine in NM, USA
- Decommissioned in Dec. 2018
- End-of-run calibration campaign data will inform the detailed design of nEXO



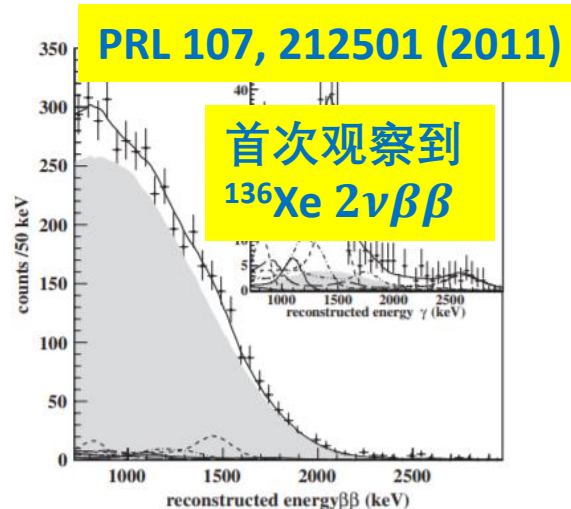
<https://www-project.slac.stanford.edu/exo/>

## nEXO:

- Next-generation 5-tonne liquid Xe TPC
- Enriched in Xe-136 at ~90%
- **Designed to go to beyond  $\sim 10^{28}$  years.**
- SNOLAB cryopit preferred location by collaboration
- Decision on funding of nEXO anticipated this summer!



<https://nexo.llnl.gov/>

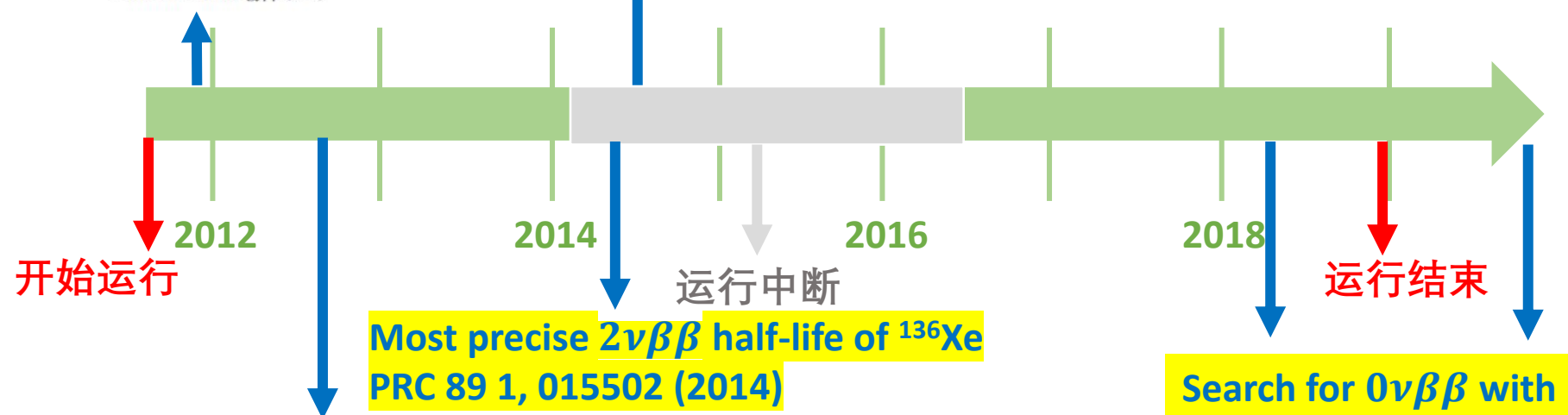


ARTICLE

Nature 510 229-234 (2014)

## Search for Majorana neutrinos with the first two years of EXO-200 data

The EXO-200 Collaboration\*



Featured in Physics

Editors' Suggestion

Access by The Library of Institute

## Search for Neutrinoless Double-Beta Decay in $^{136}\text{Xe}$ with EXO-200

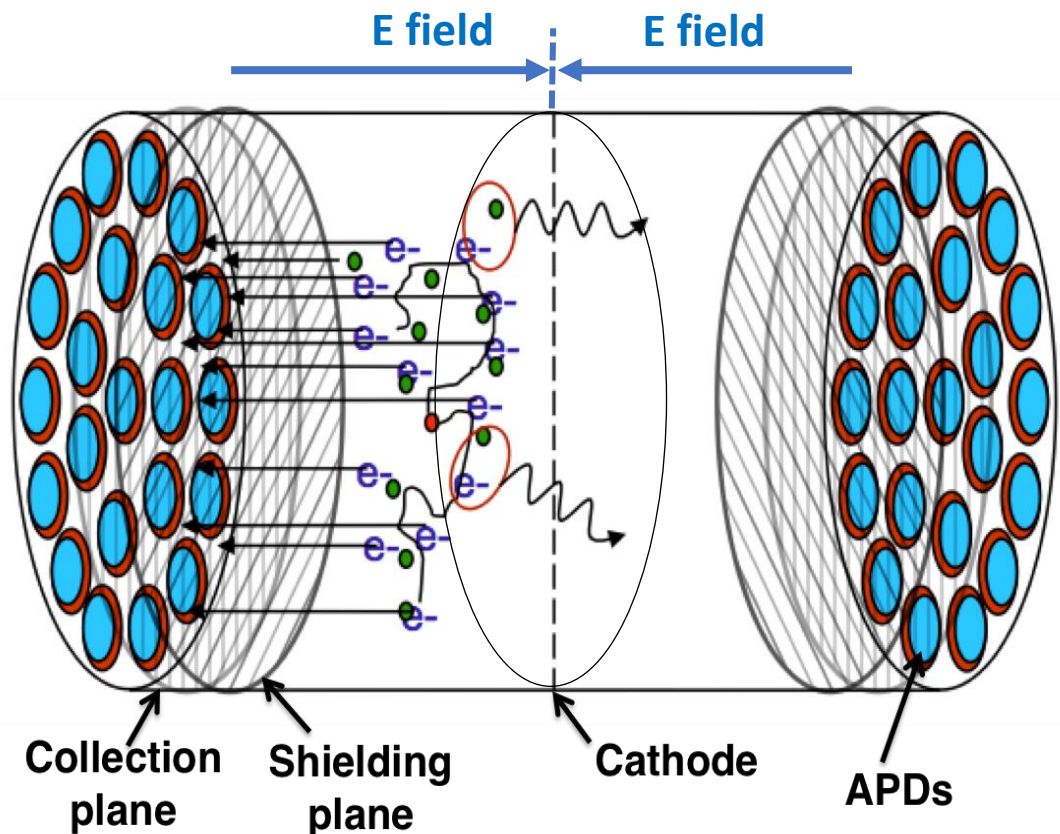
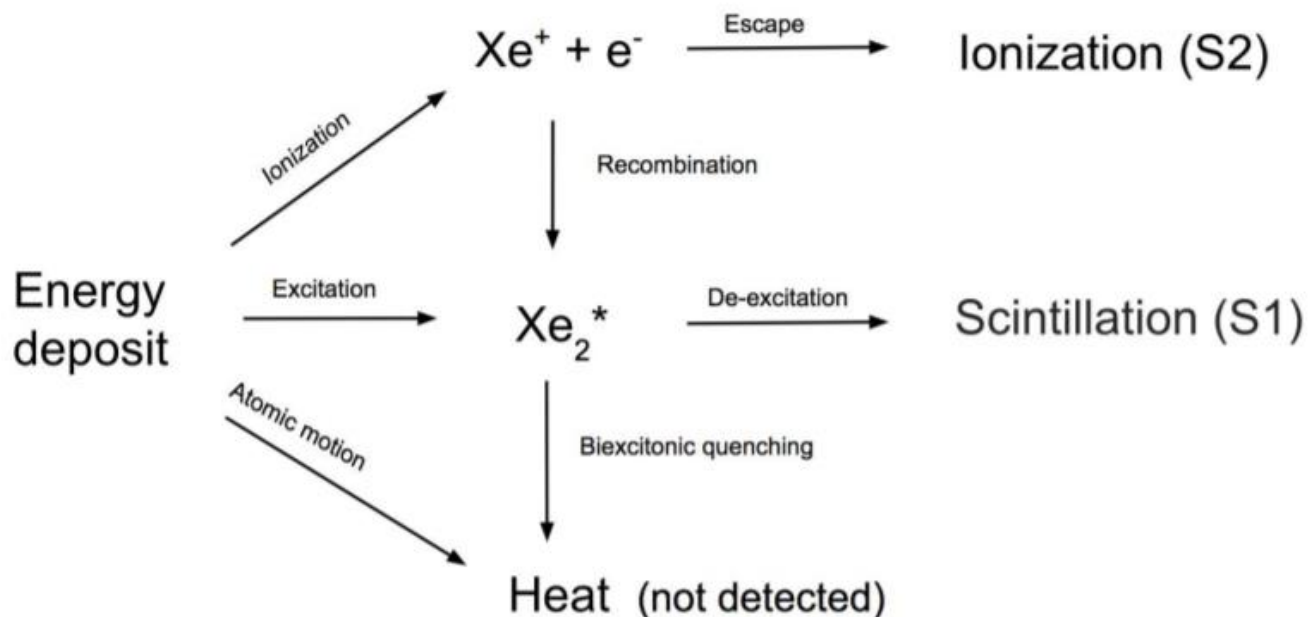
M. Auger et al. (EXO Collaboration)

Phys. Rev. Lett. 109, 032505 – Published 19 July 2012

PRL 109, 032505 (2012)

# Time Projection Chamber

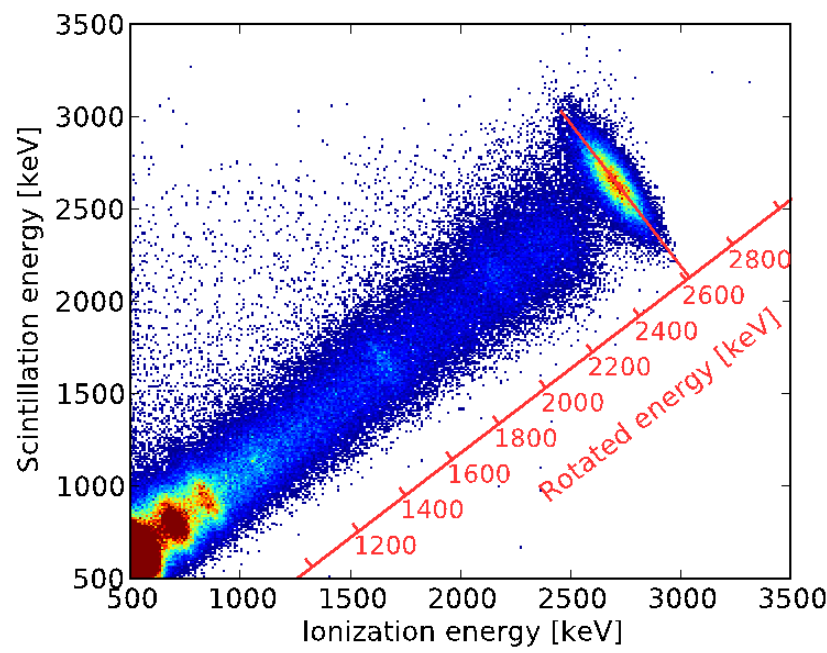
- Energy deposit in liquid xenon induced two types of signals
  - Xe atoms are ionized → electrons drift to the anode and being collected
  - Xe atoms are excited → de-excitation gives VUV photons



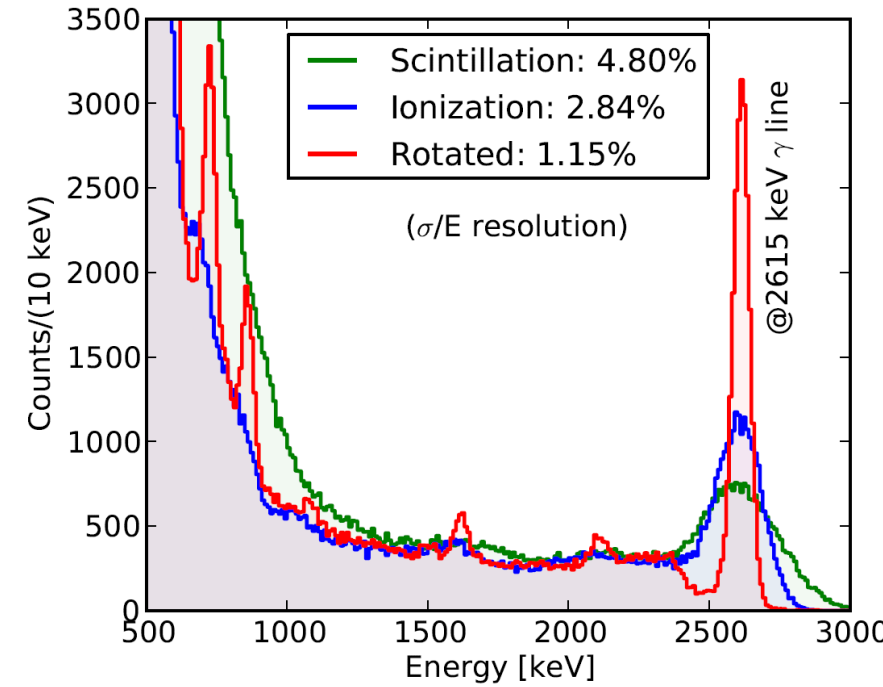
# Energy

- Using anti-correlation between charge and scintillation response
  - “Rotated” energy provides optimal resolution in the energy of interest

**Scintillation vs. ionization,  $^{228}\text{Th}$  calibration:**

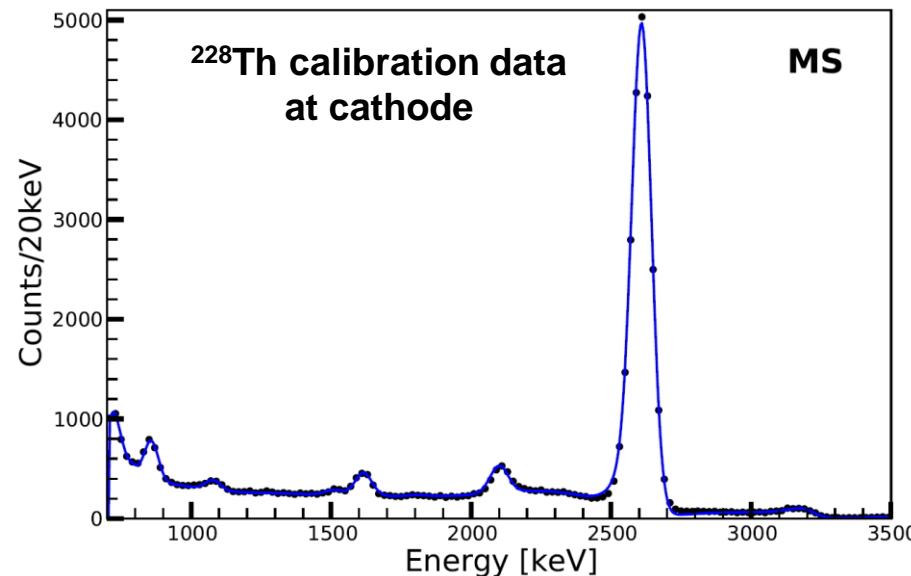
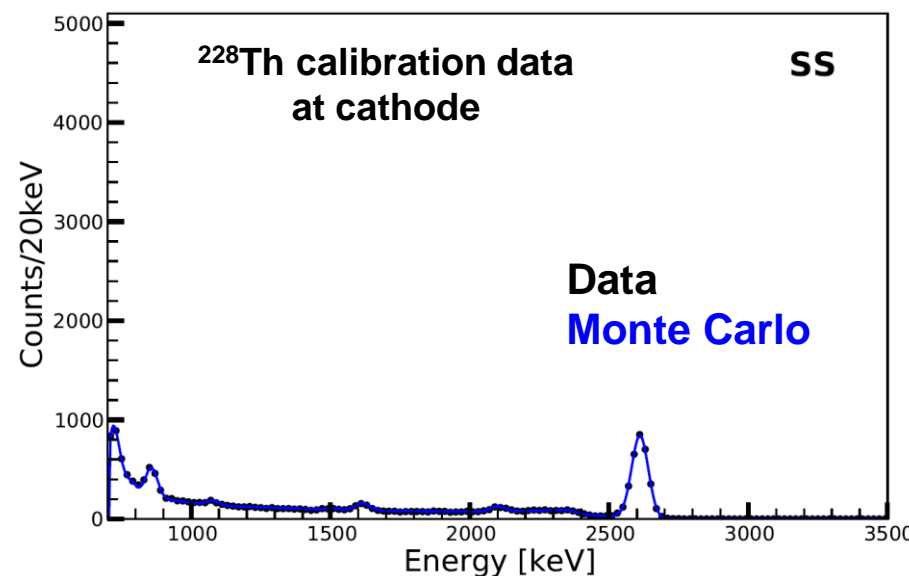
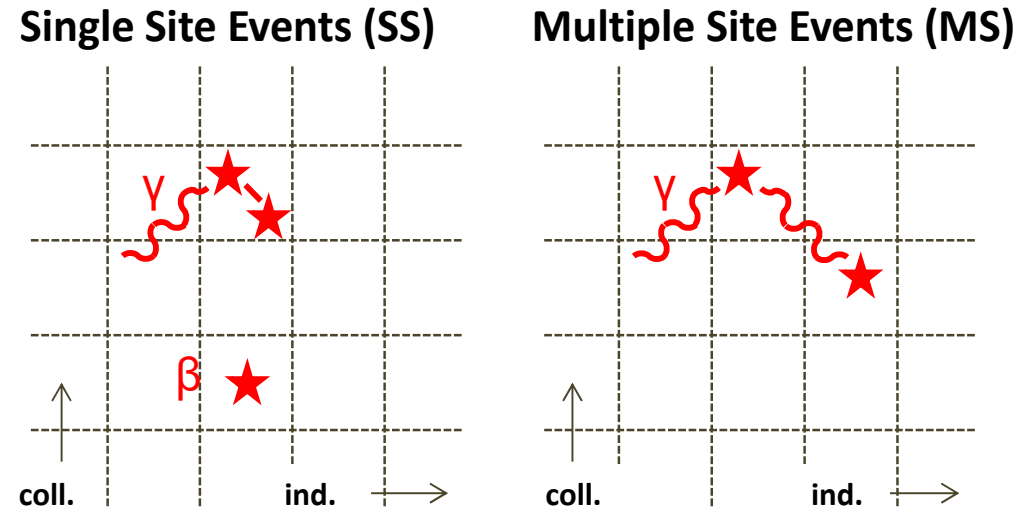


**Reconstructed energy,  $^{228}\text{Th}$  calibration:**



# 3D vertex and SS/MS classification

- X/Y (U/V) position determined by the signals in cross wire planes with 9 mm pitch
- Z position → time delay between light and charge signals
- $\beta\beta$  mostly deposits energy at single location (SS)
- $\gamma$  backgrounds deposits at multiple locations (MS)
- SS/MS classification is very powerful in background rejection



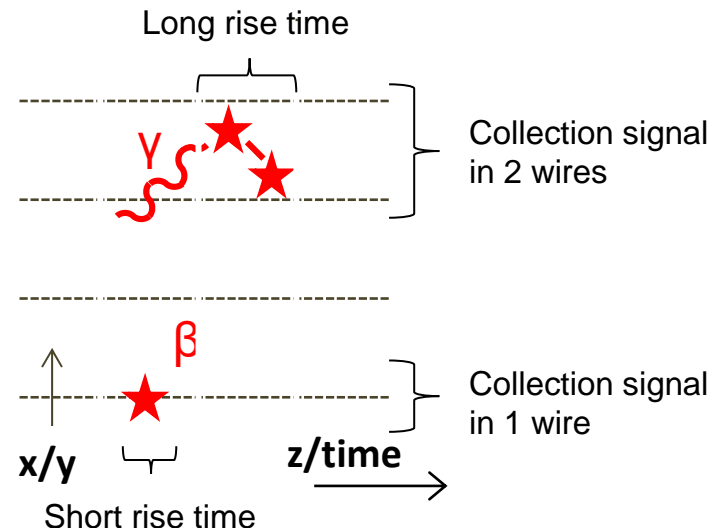
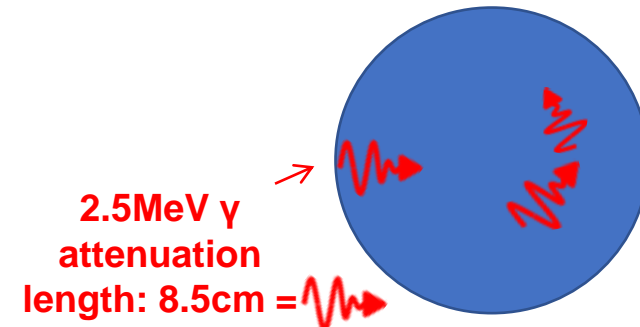
# Background Suppression: Event topology SS

- Additional discrimination in SS using *spatial distribution* and *cluster size*

- Entering  $\gamma$ -rays rate is exponentially reduced by LXe self-shielding, provides independent measurement of  $\gamma$ -backgrounds
  - standoff-distance

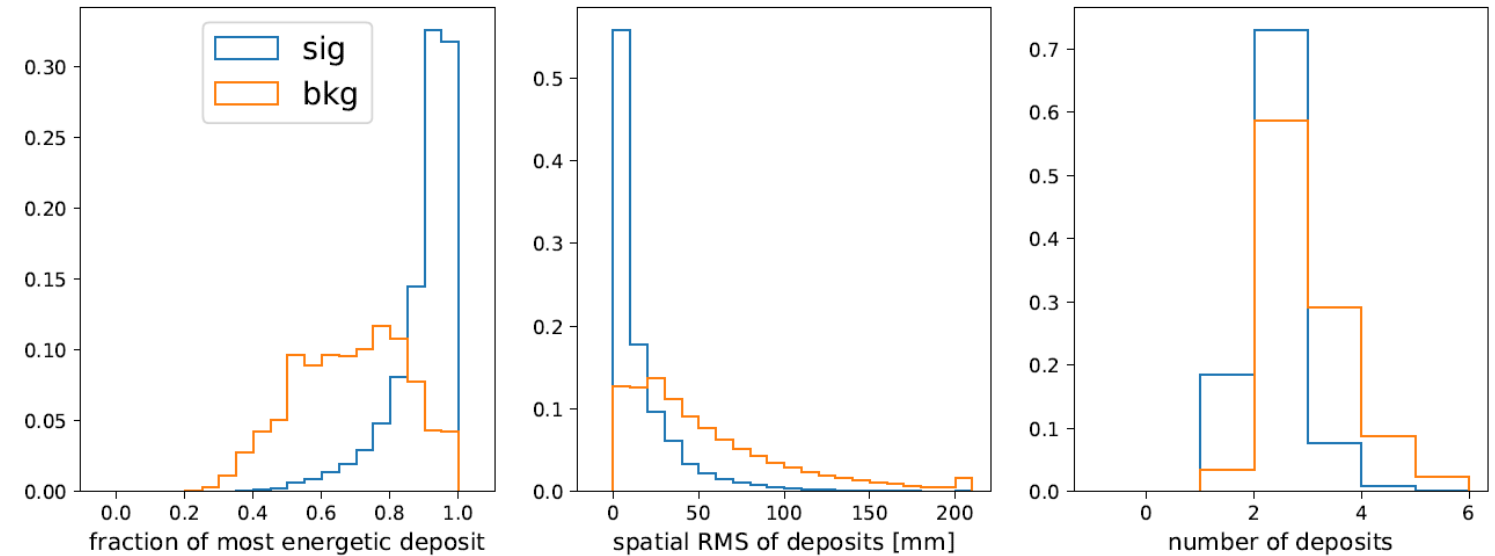
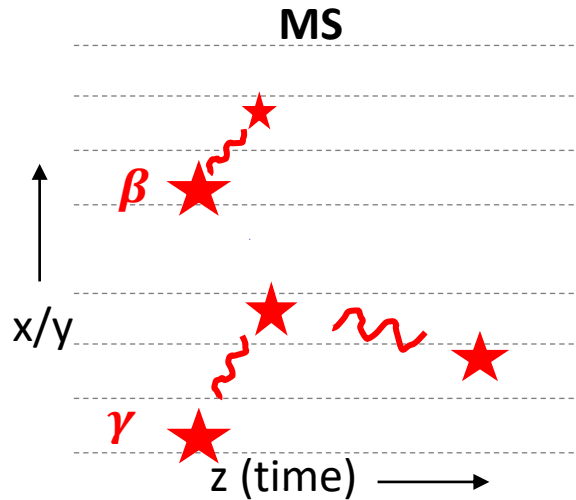
- Size of individual cluster estimated from:
  - pulse rise time (longitudinal direction)
  - number of wires with collection signal (transverse)

LXe self-shielding:



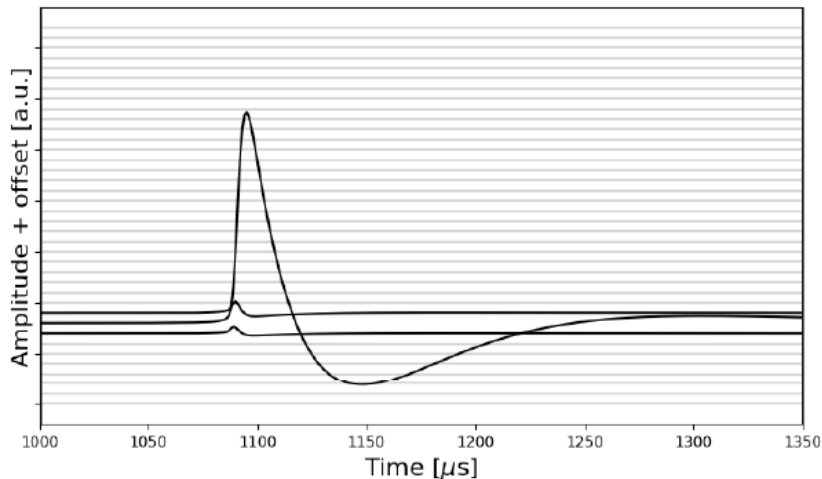
# Background Suppression: Event topology MS

- $0\nu\beta\beta$  in MS arising from small energy deposits due to bremsstrahlung, while  $\gamma$  Compton scatters
- Distinct features in number of energy deposits, energy distribution and spatial spread among deposits
- High background rejection than in SS to compensate the fact that MS is dominated by backgrounds

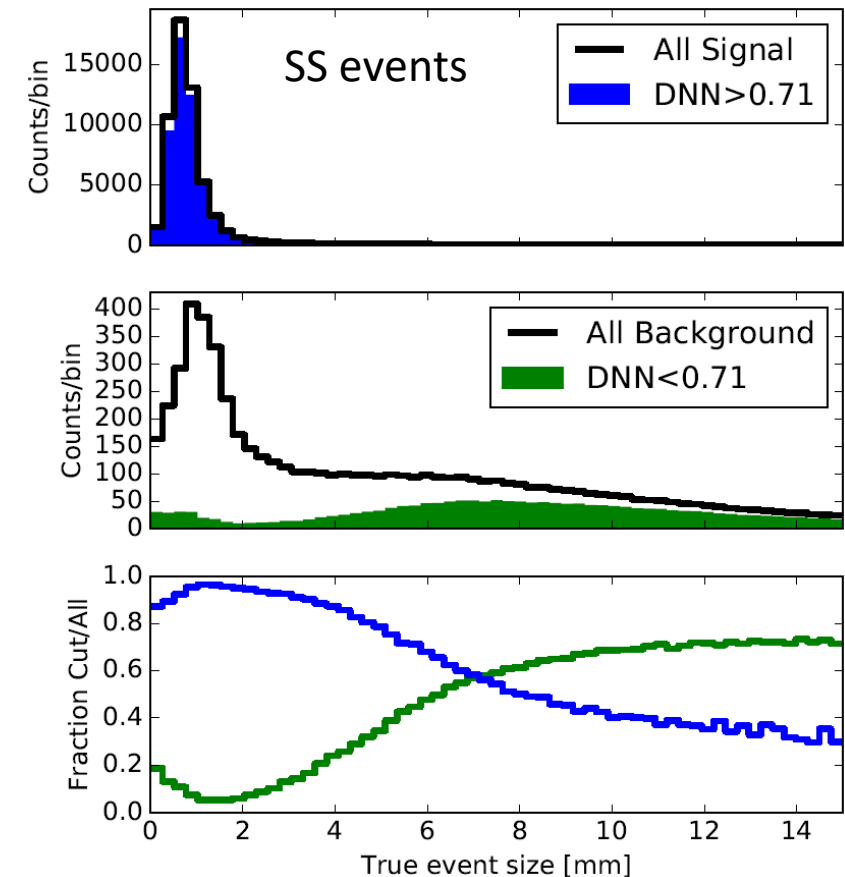


# All in DNN

- Deep neural network (DNN) based  $0\nu\beta\beta$  discriminator
- DNN trained on images built from U-wire waveforms

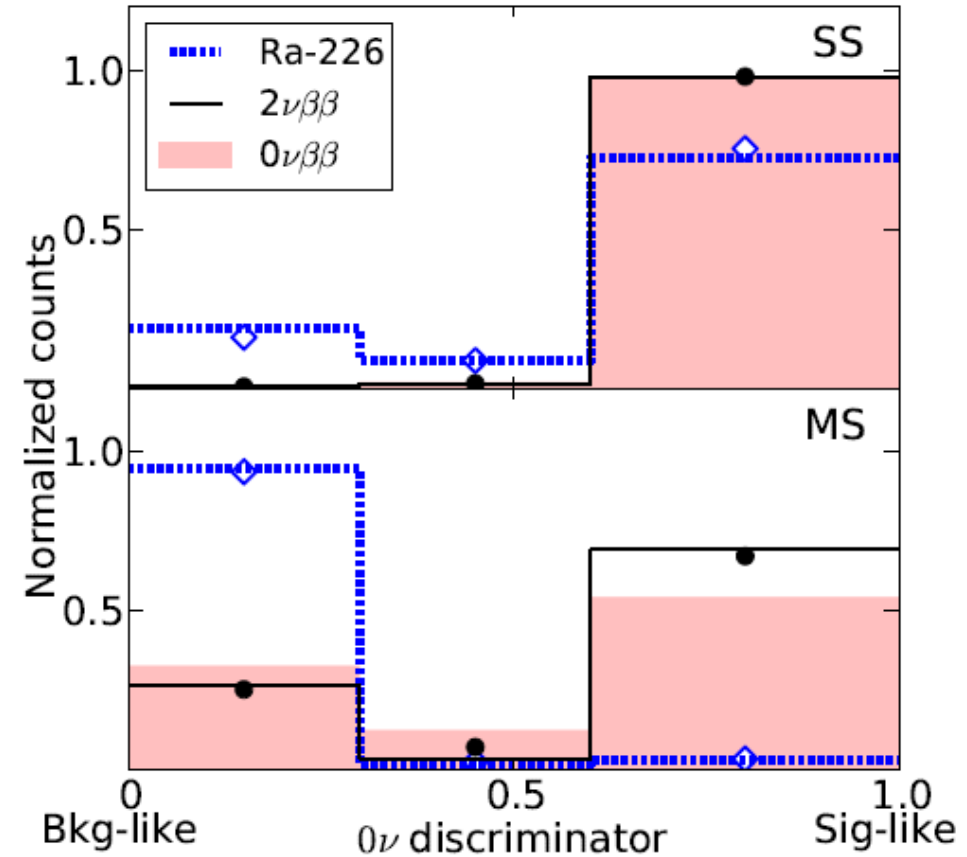


- Signal/background identification efficiency correlates with the true event size based on truth information in simulation
- Indicates the network can pick up correct features on the waveform to reconstruct event, (find wire signals, cluster signals into energy deposits), thus to discriminate signal and background

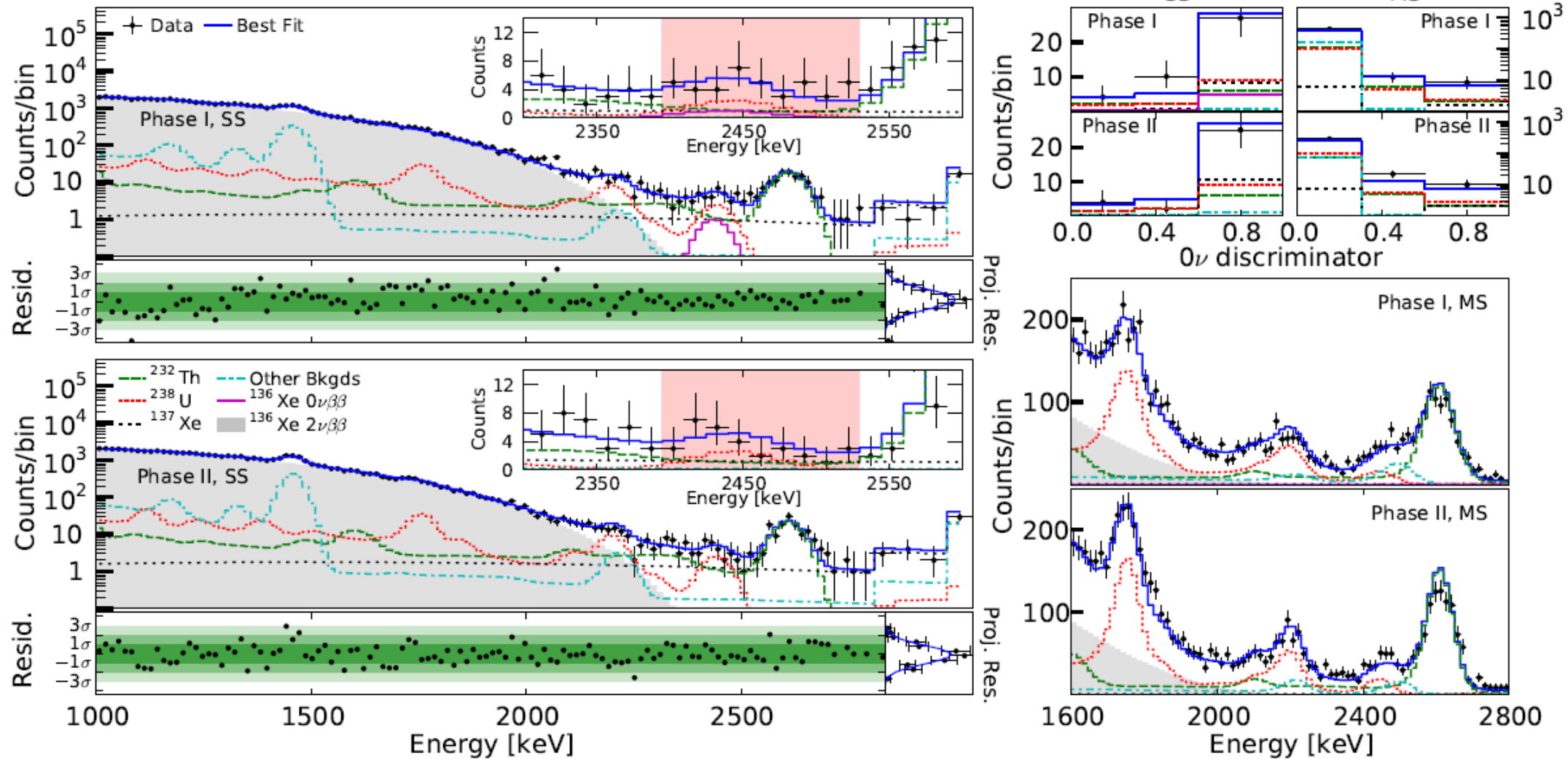


# Data/MC agreement for DNN

- Data/MC agreement validated with different data
  - $\gamma$ : Ra-226, Th-228, Co-60 calibration sources
  - $\beta$ :  $2\nu\beta\beta$  data
- Showed consistent and reasonable agreement
- Any differences in data/MC are taken into account as systematic uncertainties on normalization of backgrounds within  $Q_{\beta\beta} \pm 2\sigma$



# Multi-dimensional fit



# Results

No statistical significant signal observed

Phase I+II: 234.1 kg·yr  $^{136}\text{Xe}$  exposure  
Limit  $T_{1/2}^{0\nu\beta\beta} > 3.5 \times 10^{25}$  yr (90% C.L.)  
 $\langle m_{\beta\beta} \rangle < (93 - 286)$  meV  
Sensitivity  $5.0 \times 10^{25}$  yr

PHYSICAL REVIEW LETTERS 123, 161802 (2019)

Editors' Suggestion

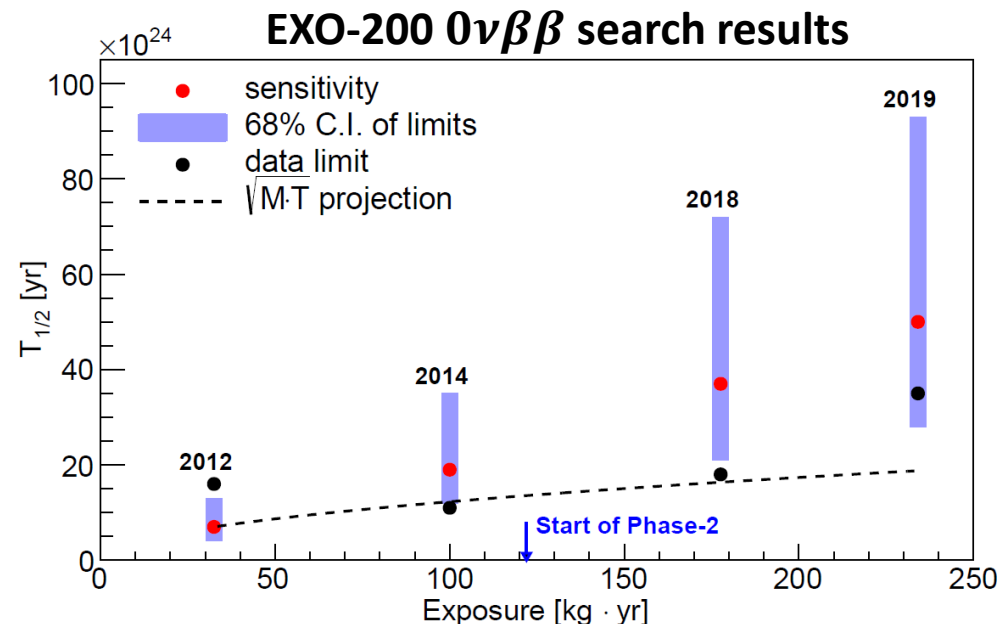
## Search for Neutrinoless Double- $\beta$ Decay with the Complete EXO-200 Dataset

G. Anton,<sup>1</sup> I. Badhrees,<sup>2,a</sup> P. S. Barbeau,<sup>3</sup> D. Beck,<sup>4</sup> V. Belov,<sup>5</sup> T. Bhatta,<sup>6</sup> M. Breidenbach,<sup>7</sup> T. Brunner,<sup>8,9</sup> G. F. Cao,<sup>10</sup> W.R. Cen,<sup>10</sup> C. Chambers,<sup>11,b</sup> B. Cleveland,<sup>12,c</sup> M. Coon,<sup>4</sup> A. Craycraft,<sup>11</sup> T. Daniels,<sup>13</sup> M. Danilov,<sup>5,d</sup> L. Darroch,<sup>8</sup> S. J. Daugherty,<sup>14</sup> J. Davis,<sup>7</sup> S. Delaquis,<sup>7,\*</sup> A. Der Mesrobian-Kabakian,<sup>12</sup> R. DeVoe,<sup>15</sup> J. Dilling,<sup>9</sup> A. Dolgolenko,<sup>5</sup> M. J. Dolinski,<sup>16</sup> J. Echevers,<sup>4</sup> W. Fairbank, Jr.,<sup>11</sup> D. Fairbank,<sup>11</sup> J. Farine,<sup>12</sup> S. Feyzakhsh,<sup>17</sup> P. Fierlinger,<sup>18</sup> D. Fudenberg,<sup>15</sup> P. Gautam,<sup>16</sup> R. Gomea,<sup>29</sup> G. Gratta,<sup>15</sup> C. Hall,<sup>19</sup> E. V. Hansen,<sup>16</sup> J. Hoessl,<sup>1</sup> M. Hughes,<sup>20</sup> A. Iverson,<sup>11</sup> A. Jamil,<sup>21</sup> C. Jessiman,<sup>2</sup> M. J. Jewell,<sup>15</sup> A. Johnson,<sup>7</sup> A. Karelina,<sup>5</sup> L. J. Kaufman,<sup>7,e</sup> T. Koffas,<sup>2</sup> R. Krücke,<sup>9</sup> A. Kuchenkov,<sup>5</sup> K. S. Kumar,<sup>22,f</sup> Y. Lan,<sup>9</sup> A. Larson,<sup>6</sup> B. G. Lenardo,<sup>15</sup> D. S. Leonard,<sup>23</sup> G. S. Li,<sup>15,f</sup> S. Li,<sup>4</sup> Z. Li,<sup>21</sup> C. Licciardi,<sup>12</sup> Y. H. Lin,<sup>16</sup> R. MacLellan,<sup>6</sup> T. McElroy,<sup>8</sup> T. Michel,<sup>1</sup> B. Mong,<sup>7</sup> D. C. Moore,<sup>21</sup> K. Murray,<sup>8</sup> O. Njoya,<sup>22</sup> O. Nusair,<sup>20</sup> A. Odian,<sup>7</sup> I. Ostrovskiy,<sup>20</sup> A. Piepke,<sup>20</sup> A. Pocar,<sup>17</sup> F. Retière,<sup>9</sup> A. L. Robinson,<sup>12</sup> P. C. Rowson,<sup>7</sup> D. Ruddell,<sup>13</sup> J. Runge,<sup>3</sup> S. Schmidt,<sup>1</sup> D. Sinclair,<sup>2,9</sup> A. K. Soma,<sup>20</sup> V. Stekhanov,<sup>5</sup> M. Tarka,<sup>17</sup> J. Todd,<sup>11</sup> T. Tolba,<sup>10</sup> T. I. Totev,<sup>8</sup> B. Veenstra,<sup>2</sup> V. Veeraraghavan,<sup>20</sup> P. Vogel,<sup>24</sup> J.-L. Vuilleumier,<sup>25</sup> M. Wagenpfeil,<sup>1</sup> J. Watkins,<sup>2</sup> M. Weber,<sup>15</sup> L. J. Wen,<sup>10</sup> U. Wichoski,<sup>12</sup> G. Wrede,<sup>1</sup> S. X. Wu,<sup>15</sup> Q. Xia,<sup>21</sup> D. R. Yahne,<sup>11</sup> L. Yang,<sup>4</sup> Y.-R. Yen,<sup>16</sup> O. Ya. Zeldovich,<sup>5</sup> and T. Ziegler<sup>1</sup>

(EXO-200 Collaboration)

## Background contribution to $Q \pm 2\sigma$

(counts)	$^{238}\text{U}$	$^{232}\text{Th}$	$^{137}\text{Xe}$	Total	Data
Phase I	12.6	10.0	8.7	$32.3 \pm 2.3$	39
Phase II	12.0	8.2	9.3	$30.9 \pm 2.4$	26



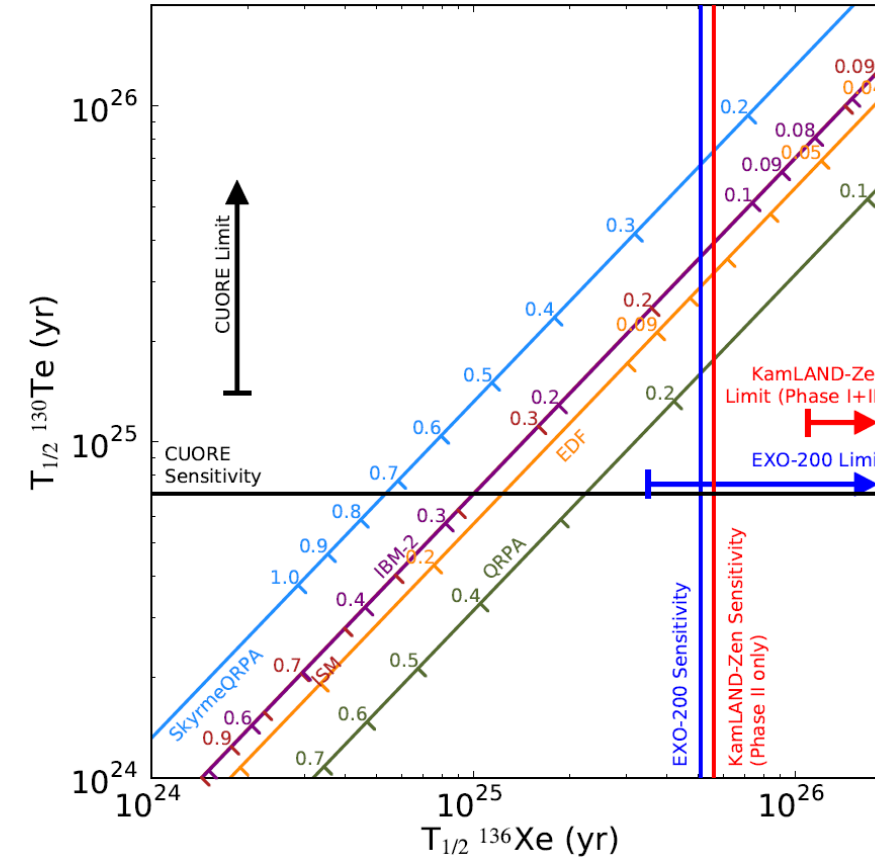
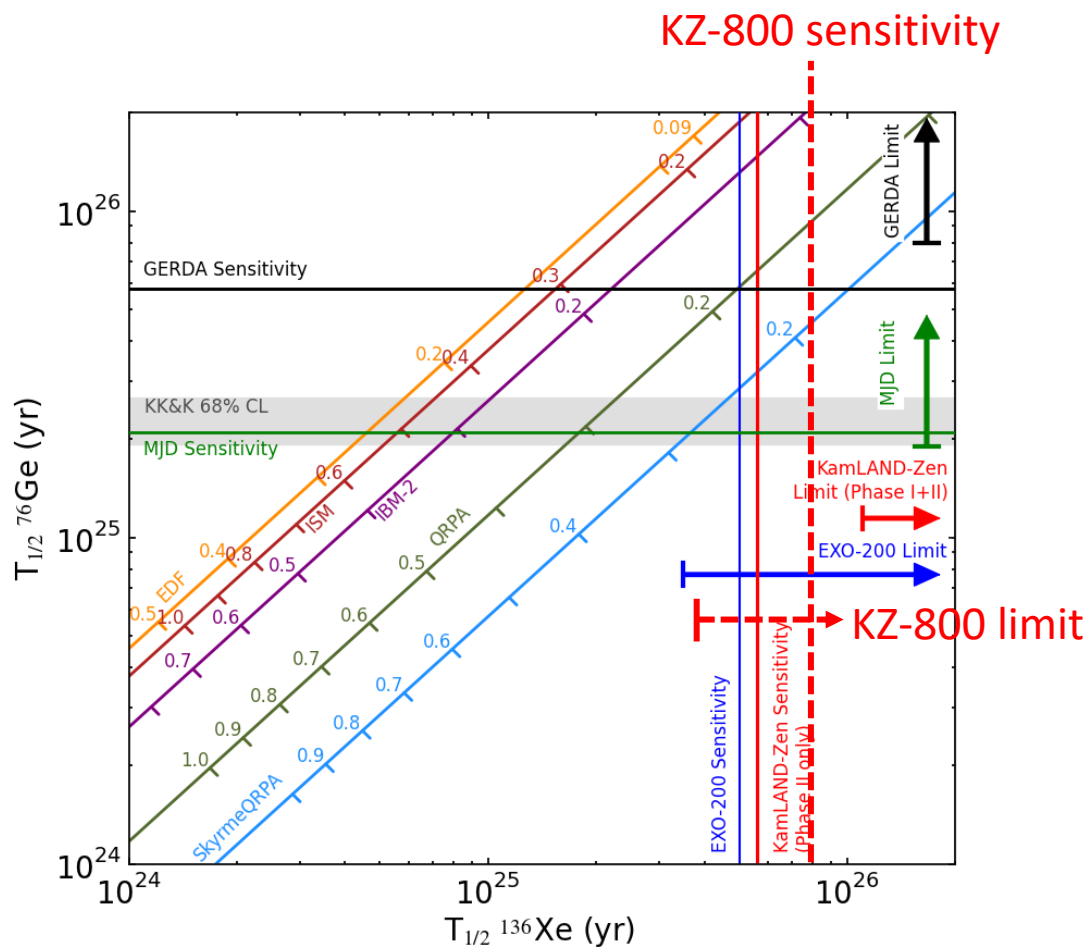
2012: *Phys. Rev. Lett.* 109 (2012) 032505

2014: *Nature* 510 (2014) 229-234

2018: *Phys. Rev. Lett.* 120, 072701 (2018)

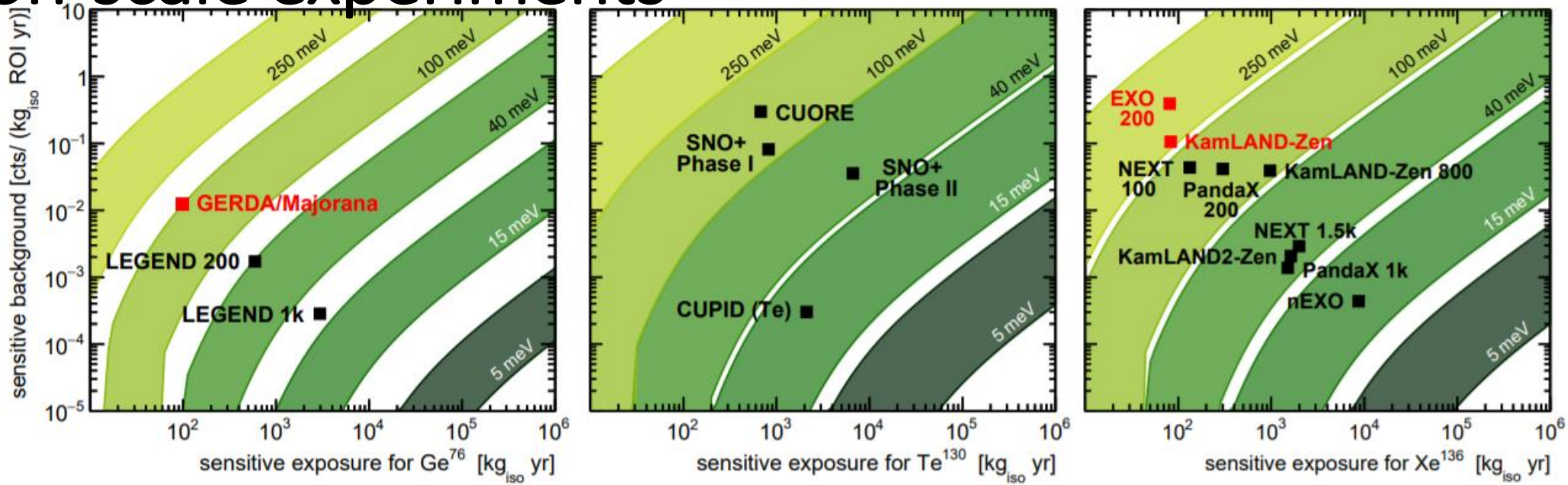
2019: *Phys. Rev. Lett.* 123 (2019) no.16, 161802 <sup>18</sup>

# Neutrino mass limits

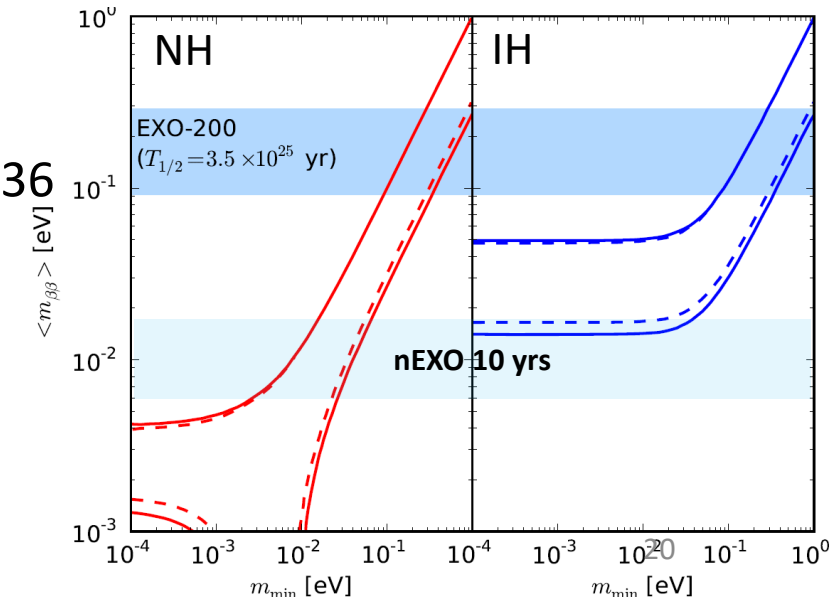


# Ton-scale experiments

Phys.Rev. D96 (2017) no.5, 053001

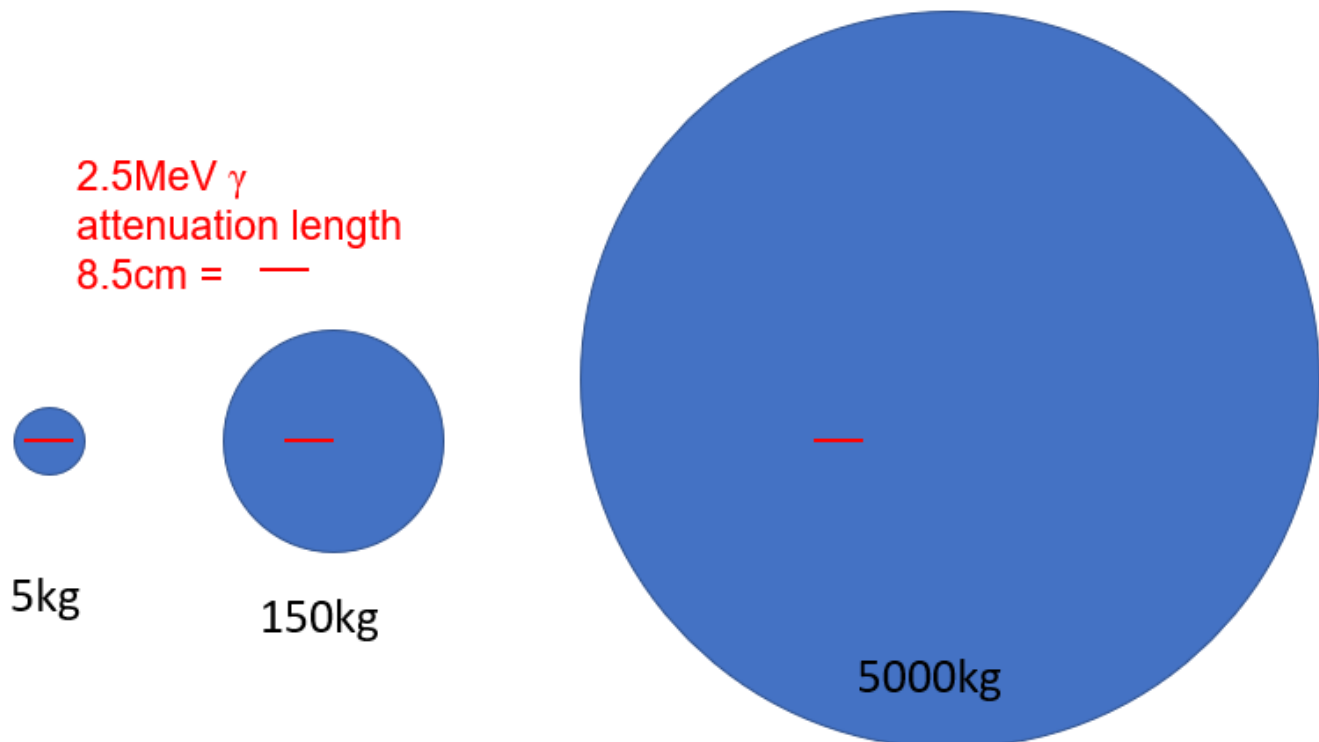
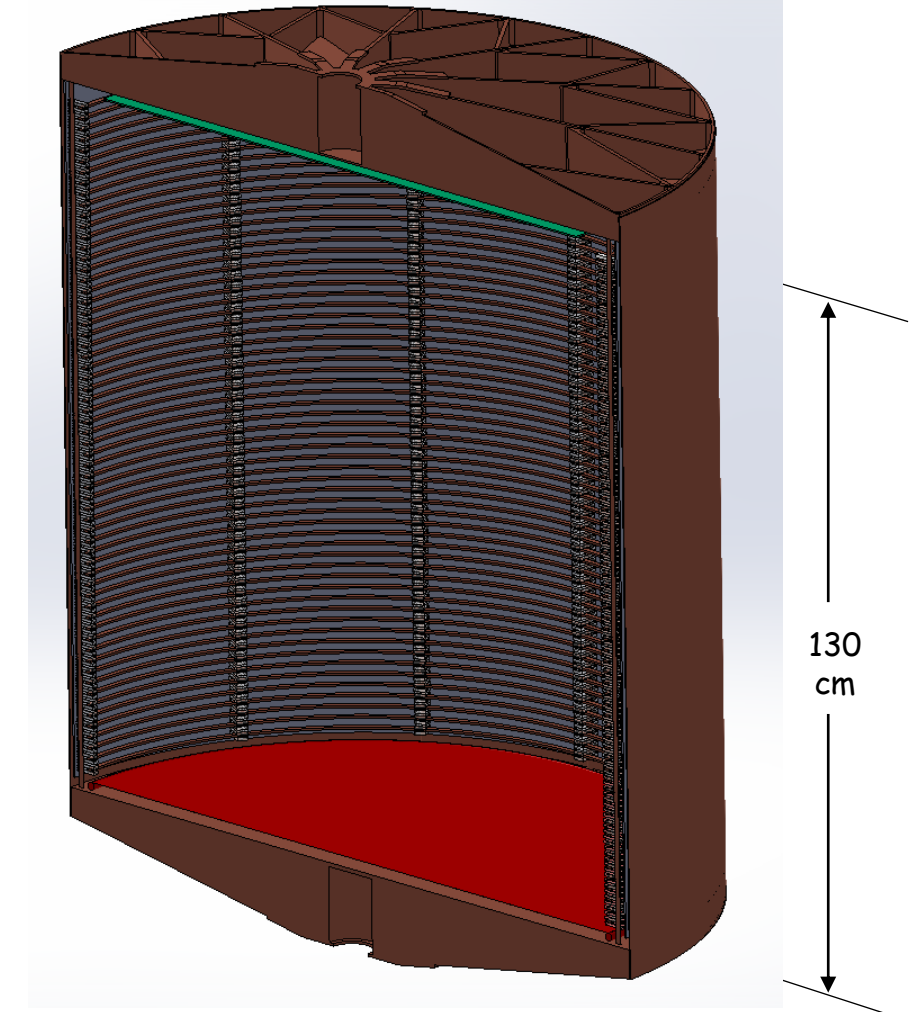
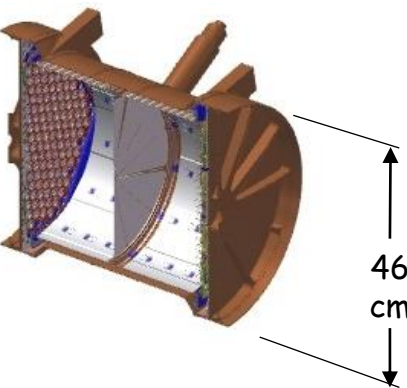


- Next generation tonne-scale experiments approaching bottom of IH or cover the entire IH
- Planned successor of EXO-200 with 5-tonne liquid xenon enriched in Xe136
- $\sim 10^{28}$  yr sensitivity to 0vbb half-life, cover the entire inverted hierarchy

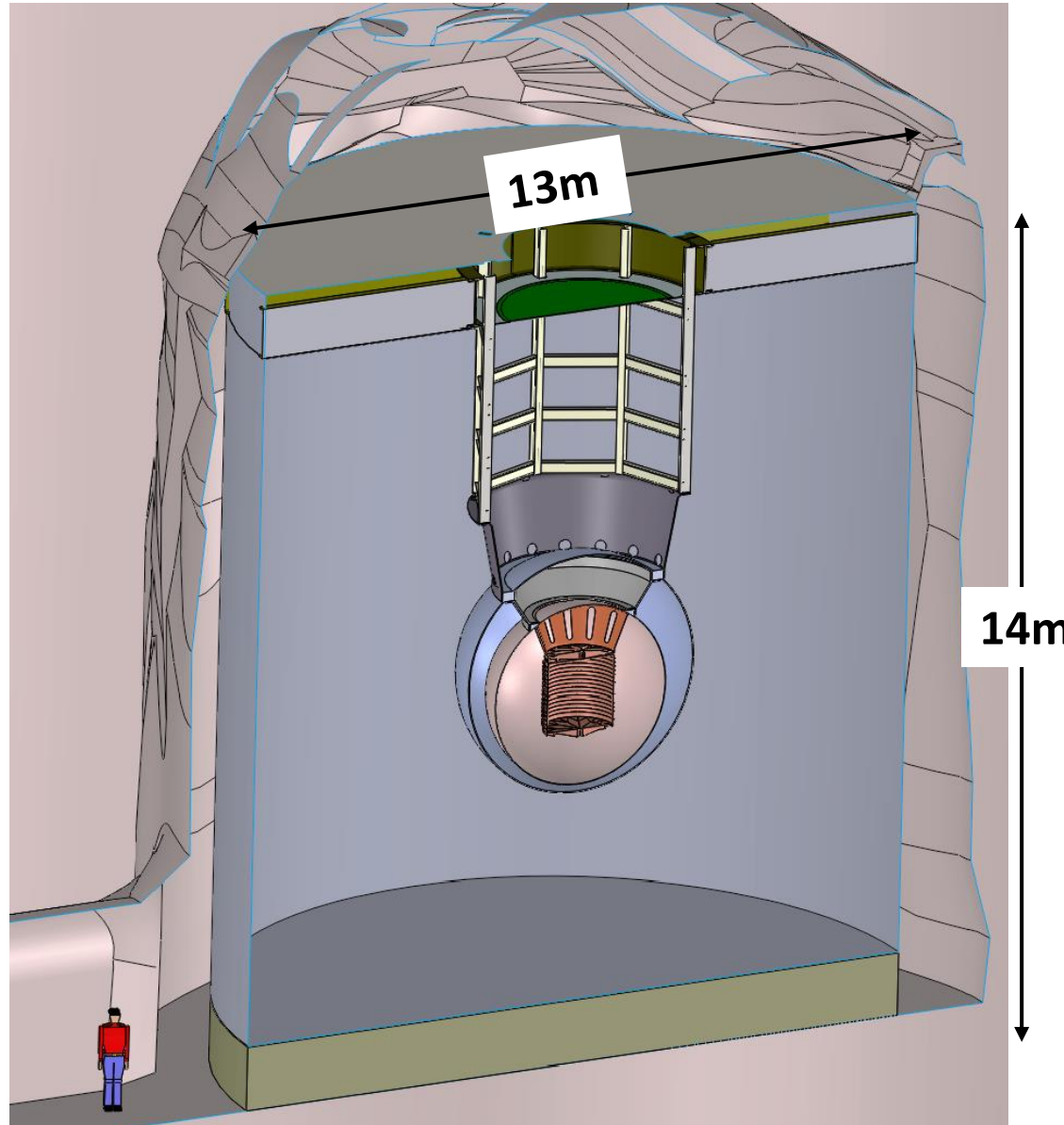


# From EXO-200 to nEXO

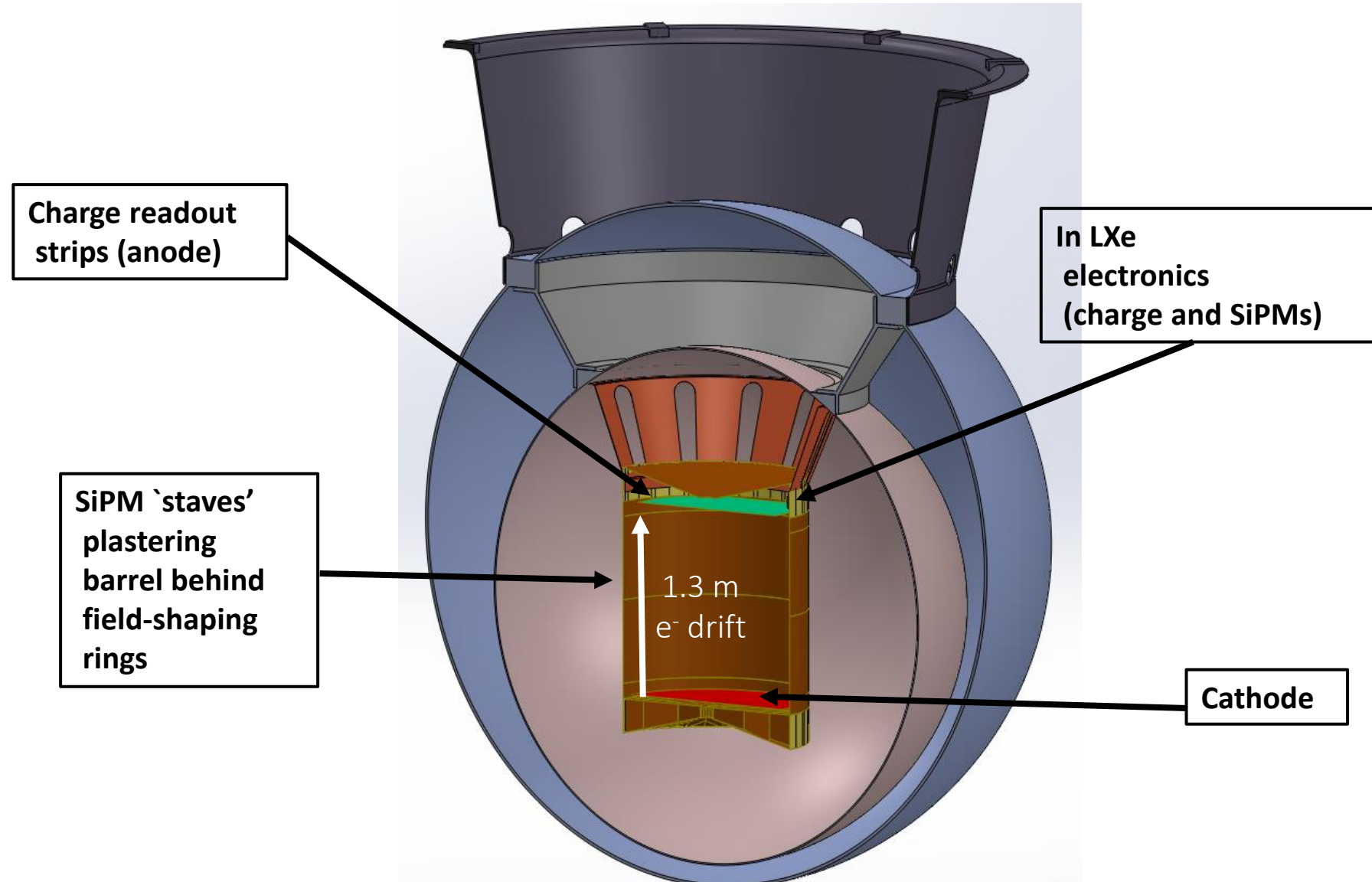
LXe mass (kg)	Diameter or length (cm)
5000	130
150	40



# Artist view of nEXO in SNOLab cryopit

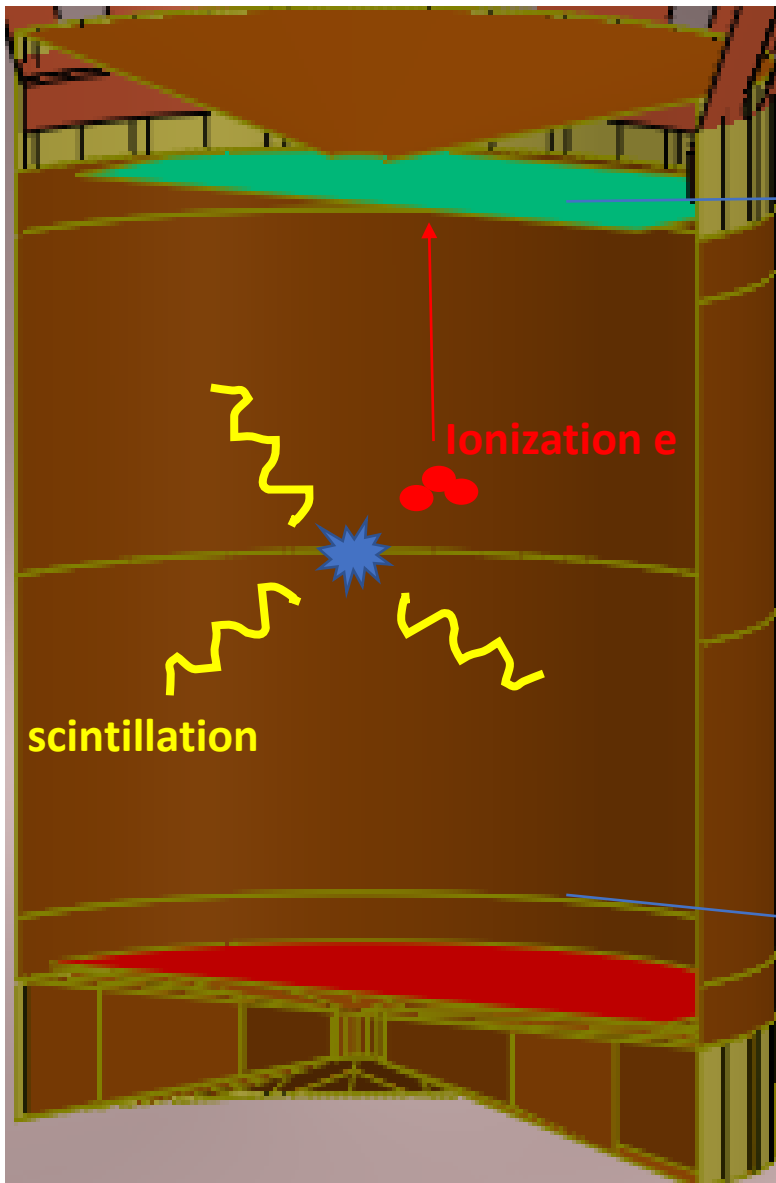


# nEXO TPC baseline design

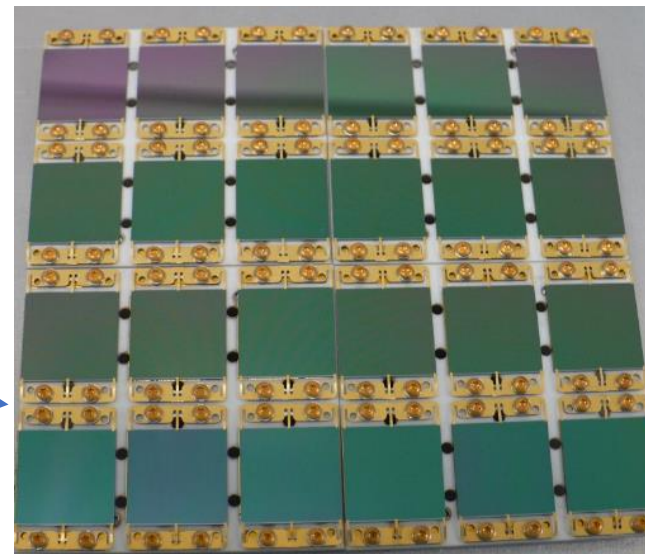
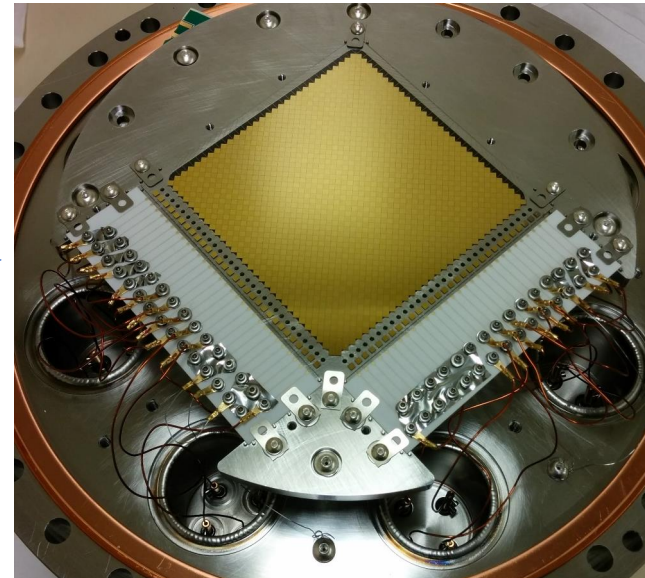


~5 tonne single phase TPC with enriched Xe136

E field

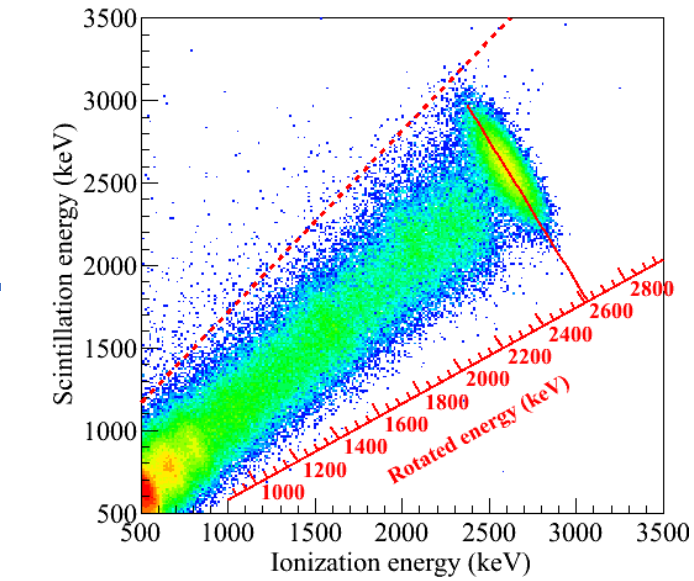


Charge tile anode for ionization  
charge collection



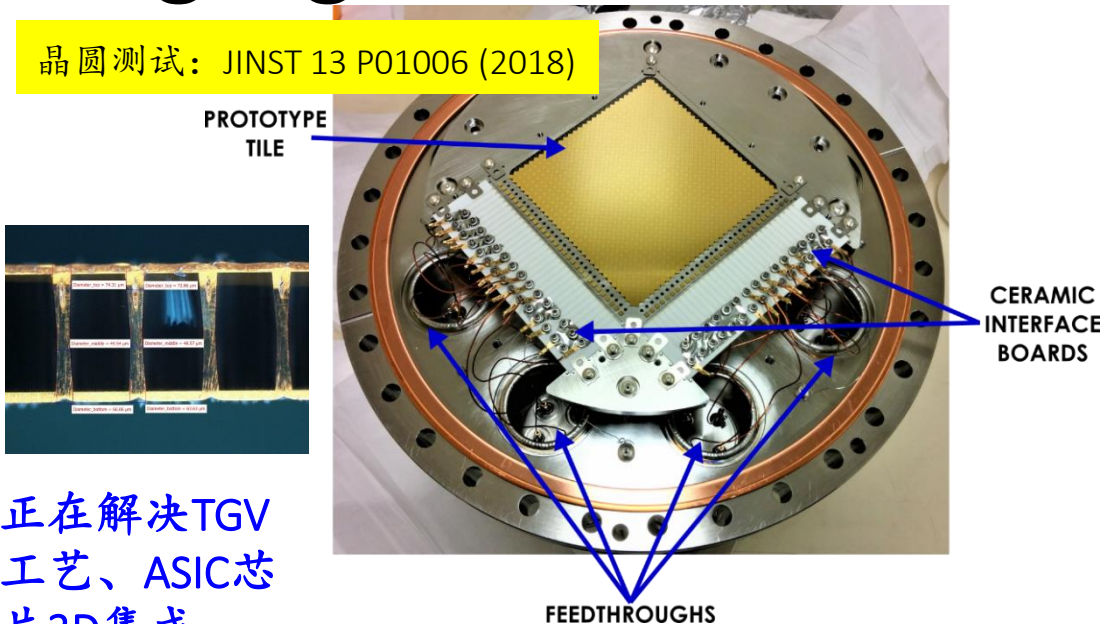
SiPM covered barrel ( $4 \text{ m}^2$ ) for  
scintillation light detection

Energy anti-correlation

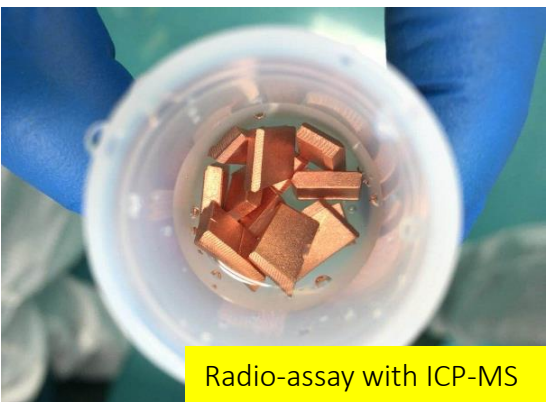


# R&D highlights at IHEP

晶圆测试: JINST 13 P01006 (2018)



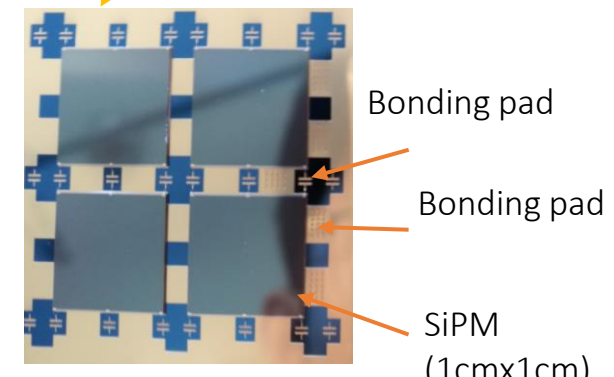
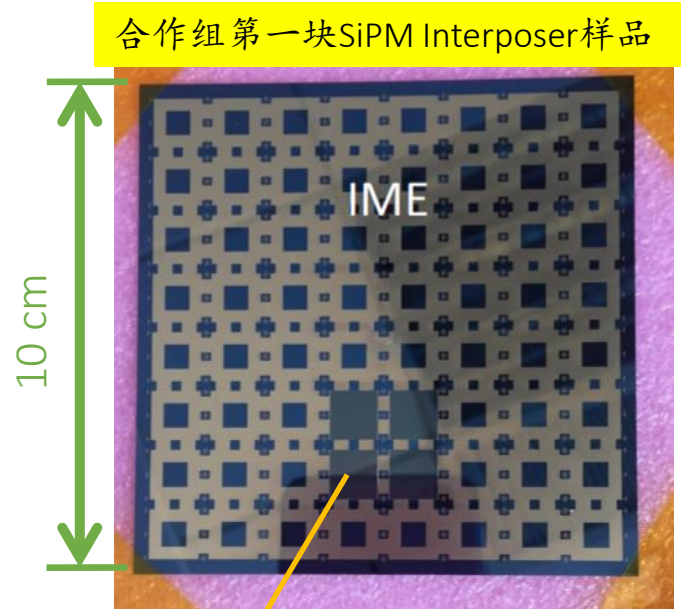
正在解决TGV  
工艺、ASIC芯  
片3D集成



Radio-assay with ICP-MS



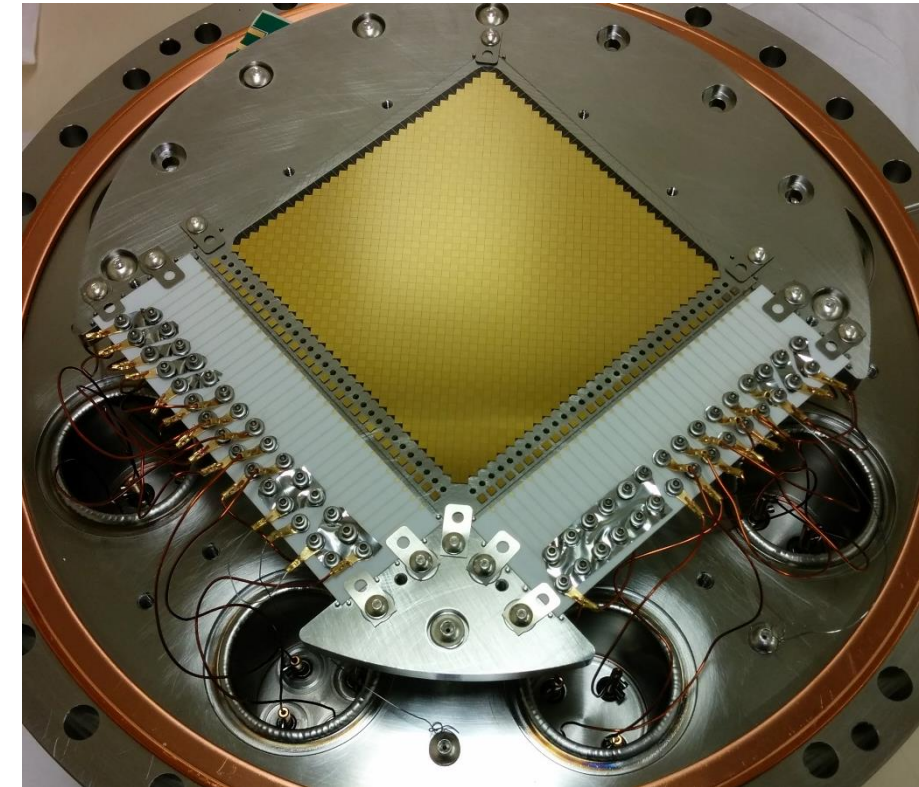
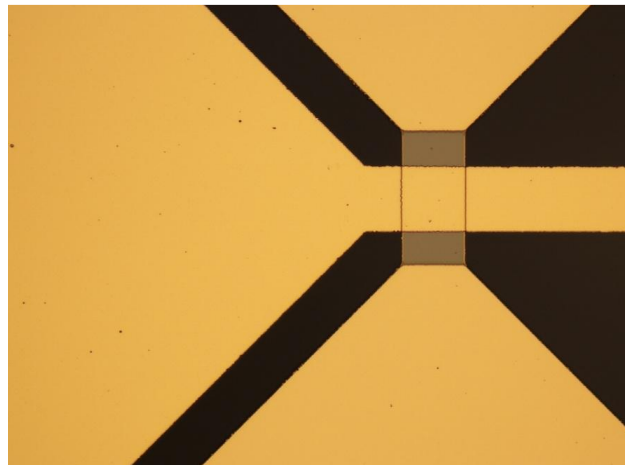
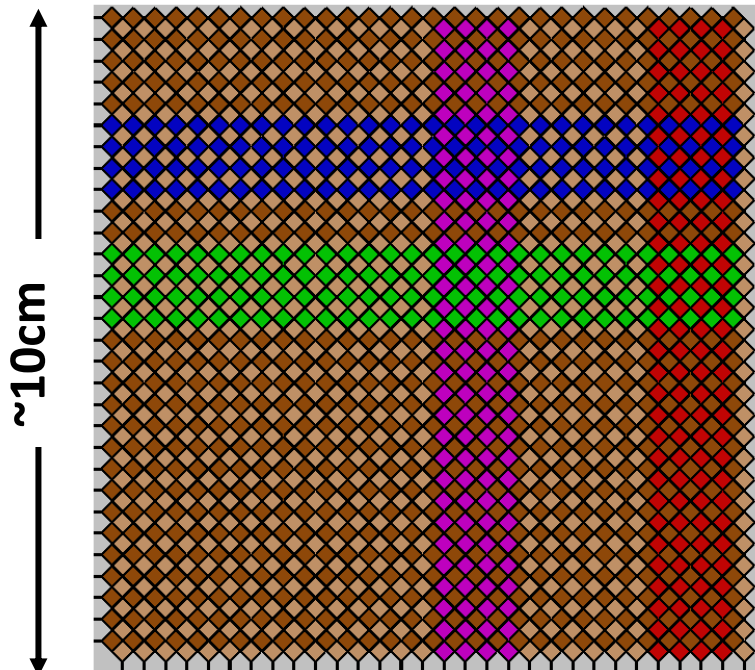
IHEP ASIC v2 测试板



nEXO: Cu中U含量检出限达到0.18 ppt  
JUNO: PPO放射性控制, 精度可到0.2~0.4 ppt

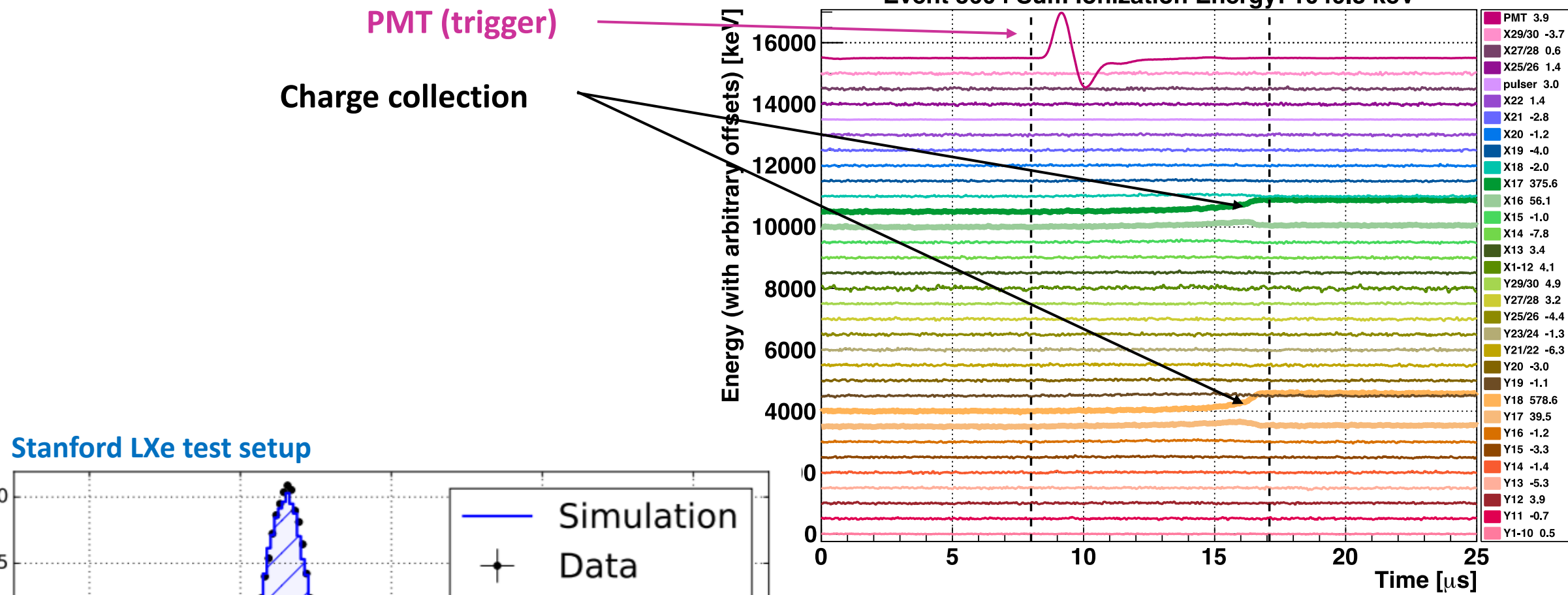
# Charge tile

- Developed by IHEP and IME
- Charge will be collected on arrays of strips fabricated onto low background dielectric wafers (baseline is silica)
  - Self-supporting/no tension
  - Built-on electronics (on back)
  - Far fewer cables
  - Ultimately more reliable, lower noise, lower activity



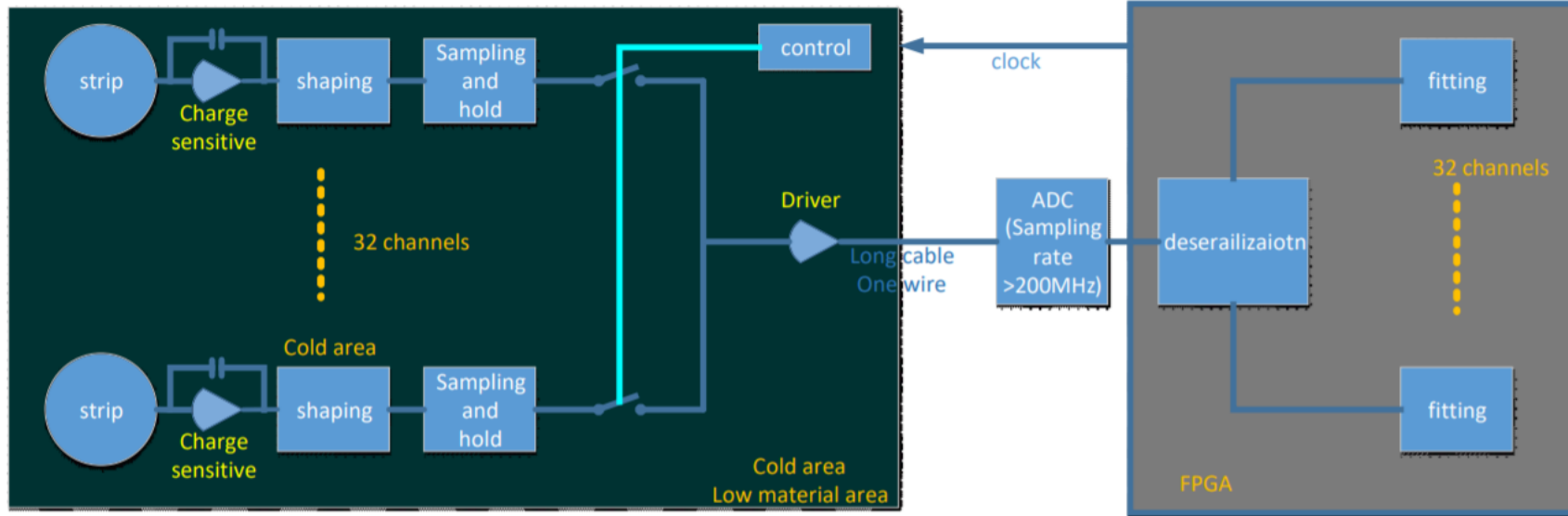
Max metallization cover  
with min capacitance

# Event 360 | Sum Ionization Energy: 1049.8 keV



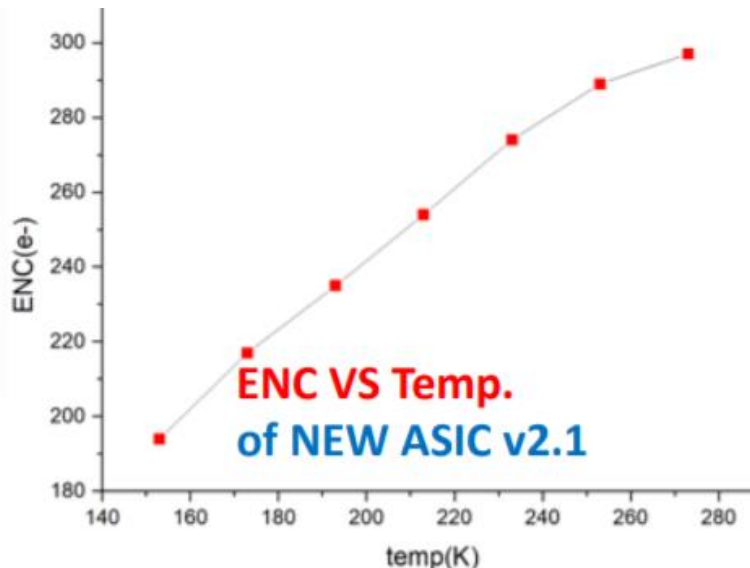
- Charge only resolution at 570 keV: 5.5%
- Consistent with the intrinsic resolution of liquid xenon

# Charge readout ASIC at IHEP

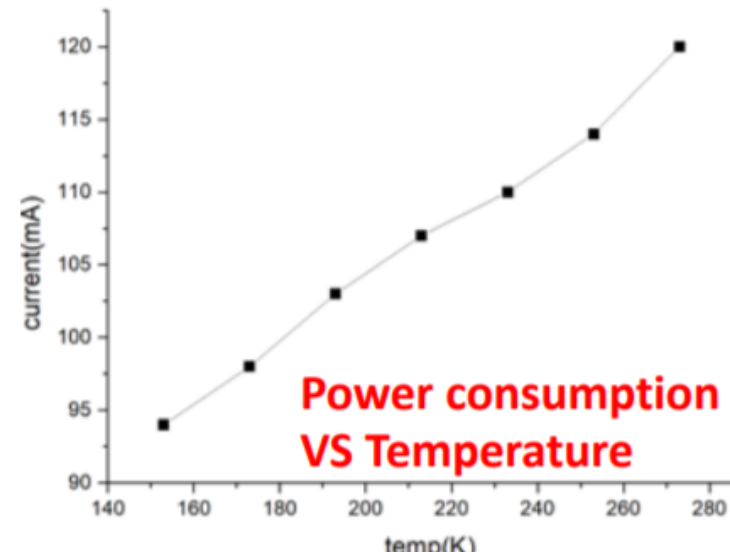


## IHEP ASIC readout design for nEXO

- Analog serial readout ASIC
- 32 channels per chip
- Low background: no extra decoupling capacitors on the board



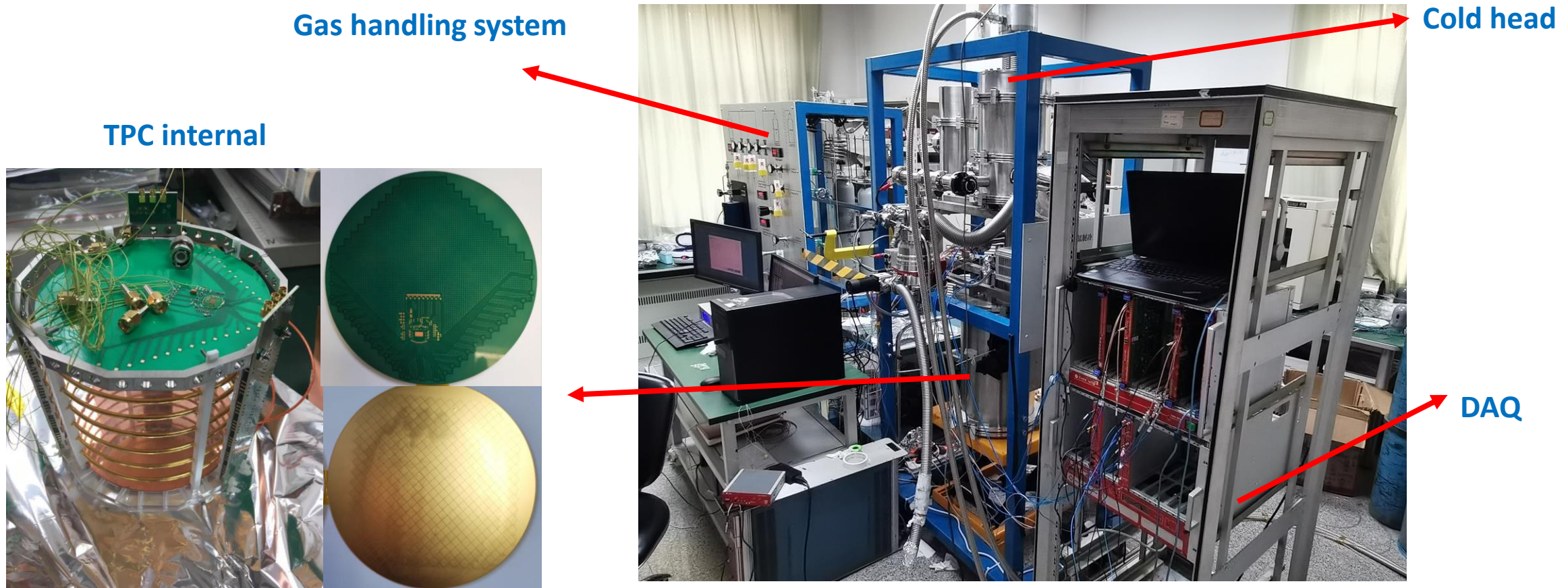
ENC VS Temp.  
of NEW ASIC v2.1



Power consumption  
VS Temperature

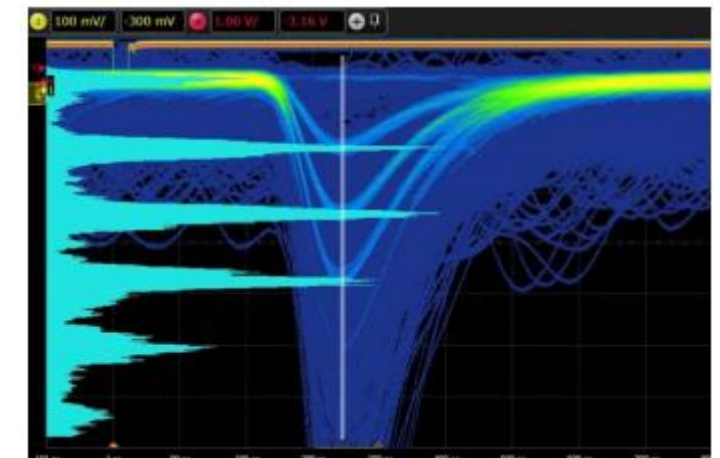
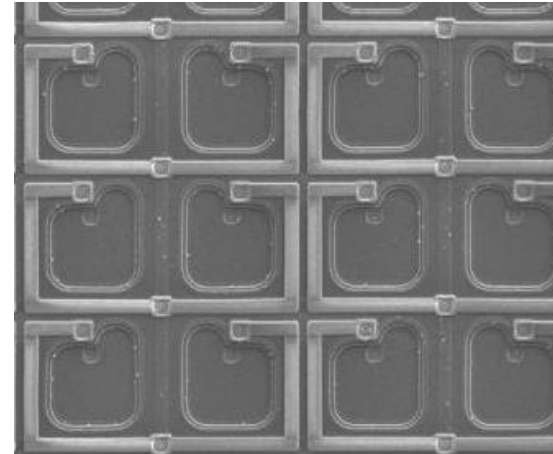
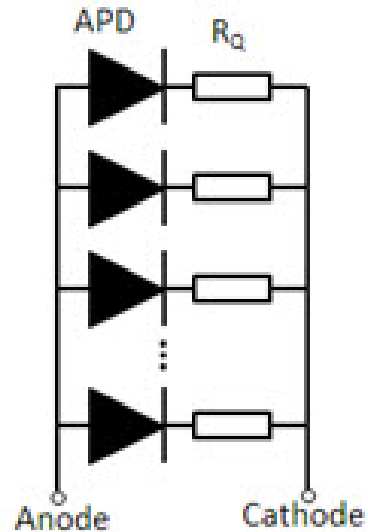
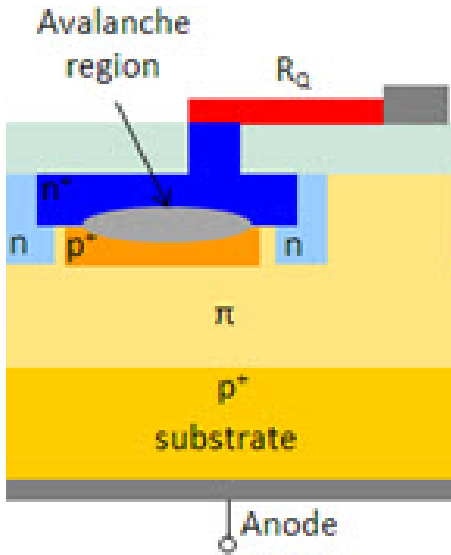
ENC down to 190  $e^-$  at 160 K

# IHEP LXe Test Setup for Charge Tile & ASIC Readout



- Major upgrades in both charge and light readout ongoing in the past several month
- Test charge tile and understand the signal shape
- Characterize ASIC performance in LXe

# Silicon photomultiplier (SiPM) for light readout



- Parallel connected arrays of SPADs operated in Geiger mode
- Passive quenching resistor stops avalanche
- “Binary” output from each pixel
- Final output is the summation of all fired pixels

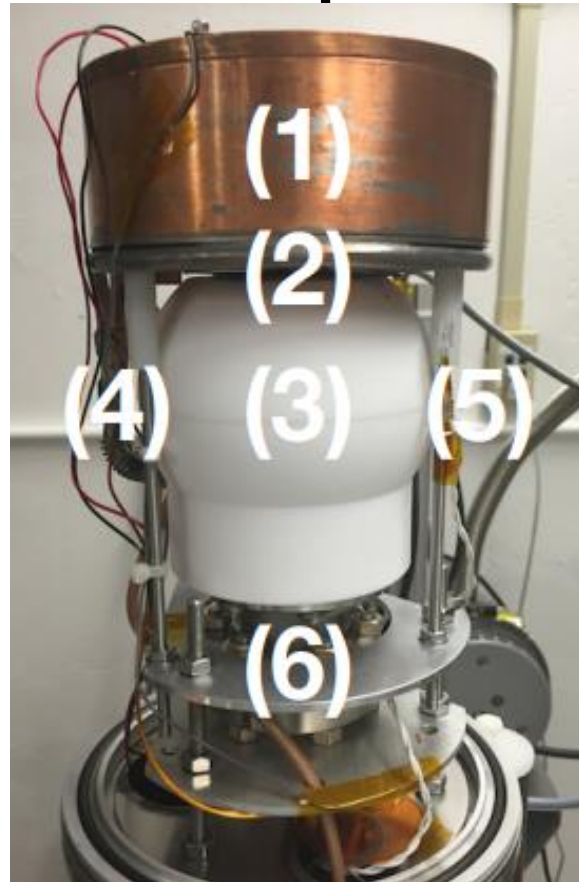
## Pros

- High gain (~1e6)
- Low radioactivity
- Immune to magnetic field
- compact

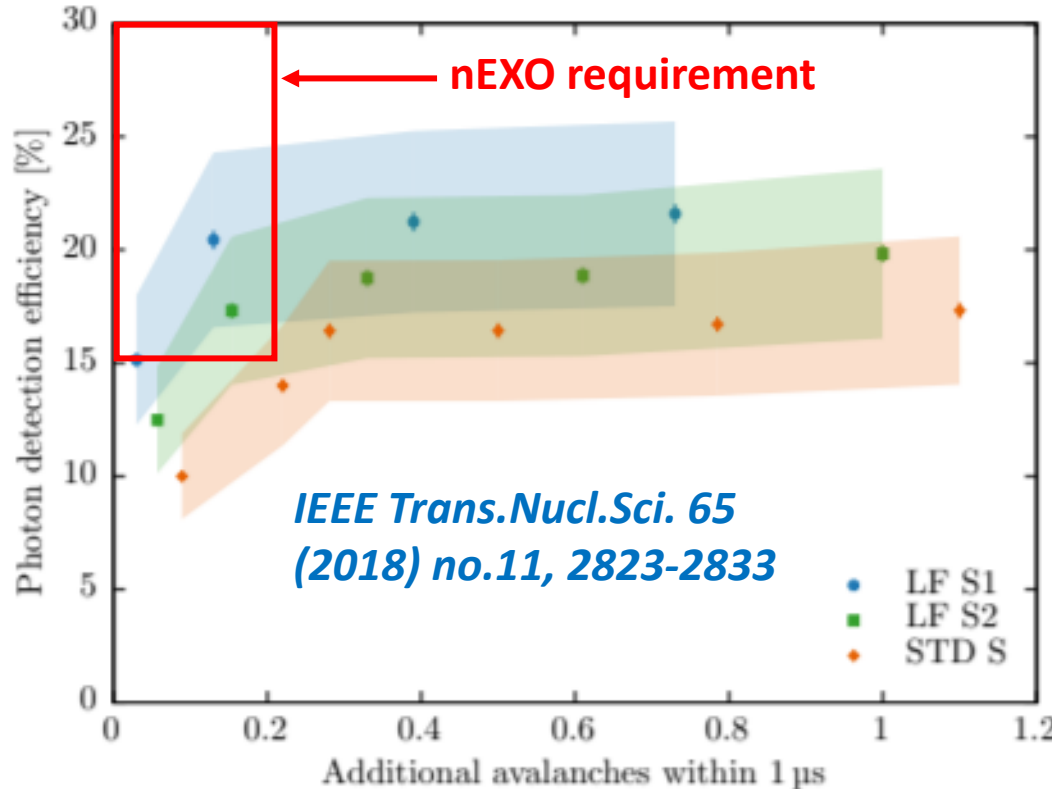
## Cons

- High dark rate (drastically reduced at cryogenic temperature though)
- After pulse and cross talk
- Large capacitance per unit area

# SiPM performance characterization



1. Detector chamber
2. Bandwidth filter
3. Reflector
4. cooling gas tube
5. LED
6. Xe scintillation light source

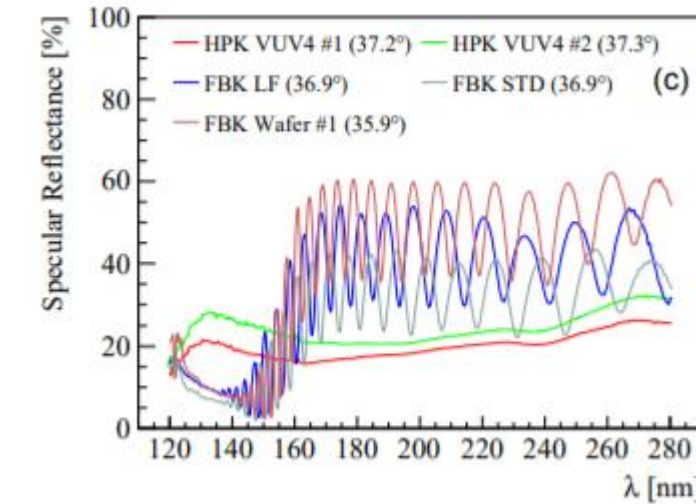
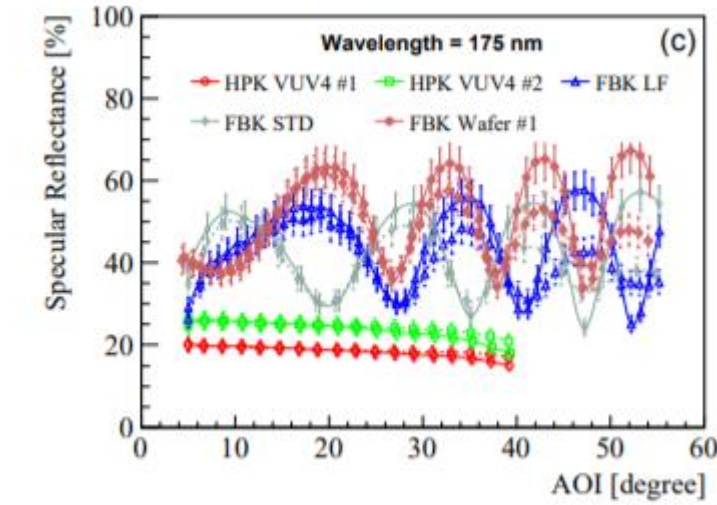
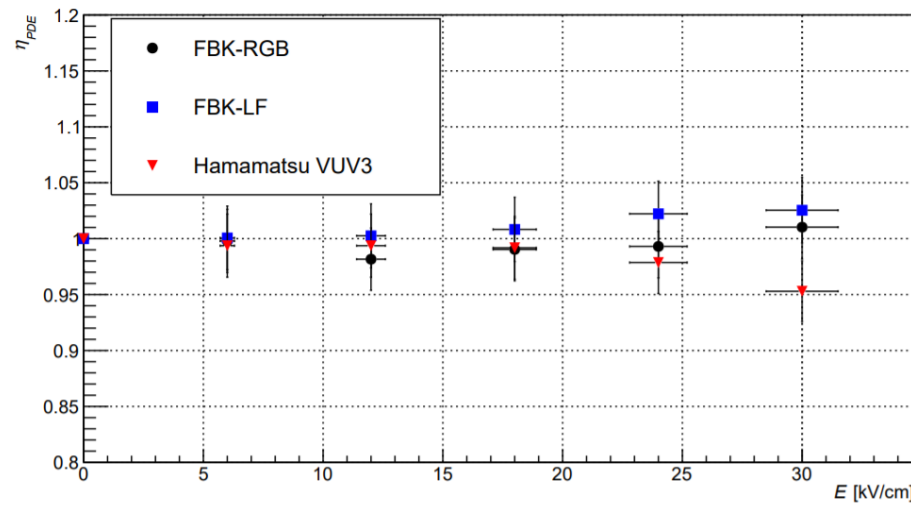
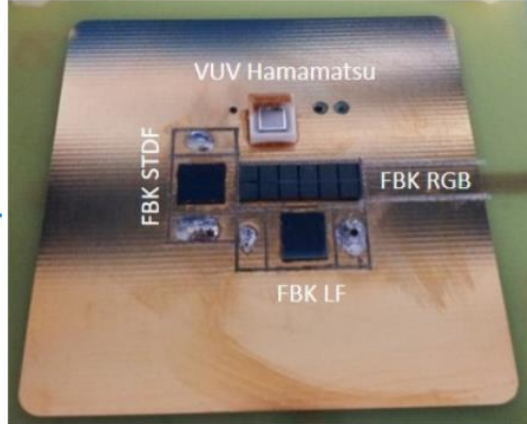
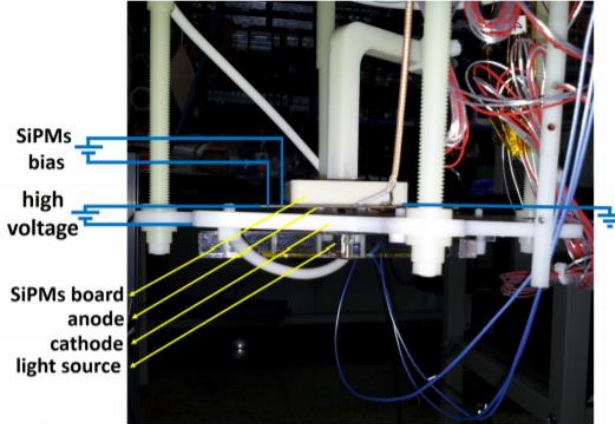


- Work closely with FBK to develop SiPM satisfying nEXO specifications
- Already found one candidate satisfying the minimum requirement

# SiPM R&D

*IEEE Trans.Nucl.Sci.* 67 (2020) 12, 2501-2510

*JINST* 13 (2018) 09, T09006

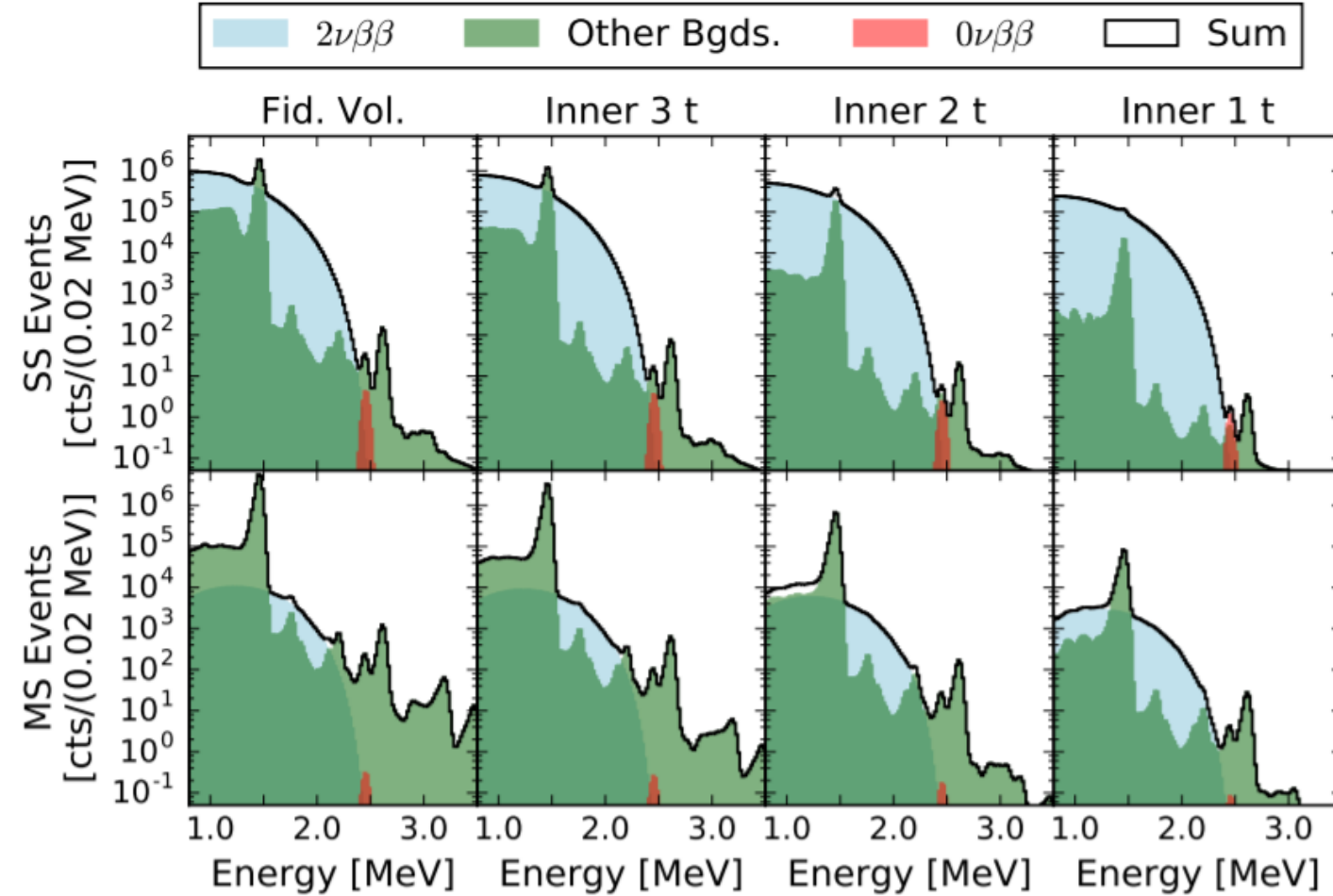


# Material assay and background model

Material	Supplier	Method	K [ppb]	Th [ppt]	U [ppt]	<sup>60</sup> Co [ $\mu$ Bq/kg]
Copper	Aurubis	ICPMS/Ge/GDMS	<0.7	0.13±0.06	0.26±0.01	<3.2
Sapphire	GTAT	NAA	9.5±2.0	6.0±1.0	<8.9	-
Quartz	Heraeus	NAA	0.55±0.04	<0.23	<1.5	-
SiPM	FBK	ICPMS/NAA	<8.7	0.45±0.12	0.86±0.05	-
Epoxy*	Epoxies Etc.	NAA	<20	<23	<44	-
Kapton*	Nippon Steel Cables	ICPMS	-	<2.3 pg/cm <sup>2</sup>	4.7±0.7 pg/cm <sup>2</sup>	-
HFE*	3M HFE-7000	NAA	<0.6	<0.015	<0.015	-
Carbon Fiber	Mitsubishi Grafil	Ge	550±51	58±19	19±8	-
ASICs	BNL	ICPMS	-	25.7±0.7	13.2±0.1	
Titanium	TIMET	Ge	<3.3	57±5	<7.3	-
Water	SNOLAB	Assumed	<1000	<1	<1	-

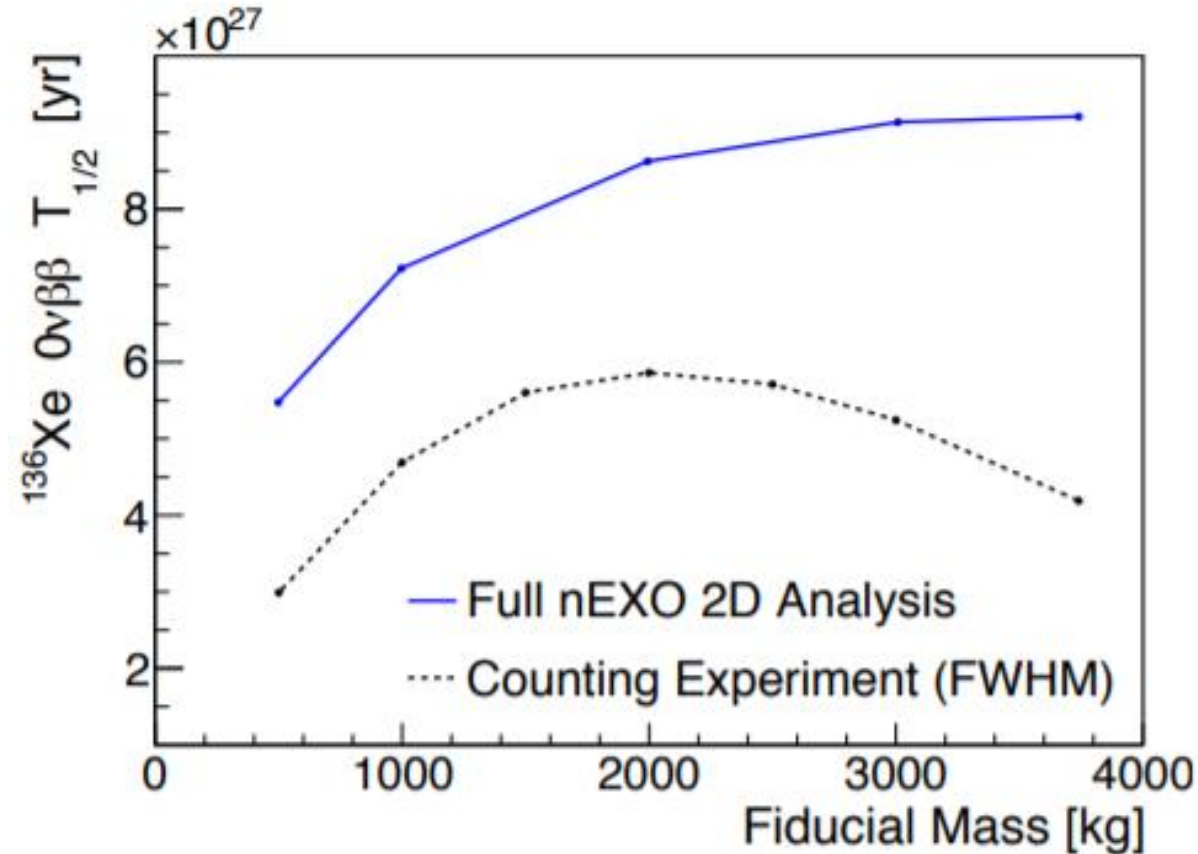
Component	Nuclides Simulated	Material	Mass or
			Surface Area
Outer Cryostat	<sup>238</sup> U, <sup>232</sup> Th, <sup>40</sup> K	Carbon Fiber	1774 kg
Inner Cryostat	<sup>238</sup> U, <sup>232</sup> Th, <sup>40</sup> K	Carbon Fiber	338 kg
Inner Cryostat Liner	<sup>238</sup> U, <sup>232</sup> Th	Titanium	161.4 kg
HFE	<sup>238</sup> U, <sup>232</sup> Th	HFE-7000	32700 kg
TPC Vessel	<sup>238</sup> U, <sup>232</sup> Th	Copper	553.4 kg
Cathode	<sup>238</sup> U, <sup>232</sup> Th	Copper	13.02 kg
Field Rings (FR)	<sup>238</sup> U, <sup>232</sup> Th	Copper	73.2 kg
FR Support Leg	<sup>238</sup> U, <sup>232</sup> Th, <sup>40</sup> K	Sapphire	0.94 kg
FR Support Spacer	<sup>238</sup> U, <sup>232</sup> Th, <sup>40</sup> K	Sapphire	2.21 kg
SiPM	<sup>238</sup> U, <sup>232</sup> Th, <sup>40</sup> K	SiPM	4.69 kg
SiPM Support	<sup>238</sup> U, <sup>232</sup> Th	Copper	136.4 kg
SiPM Module Backing	<sup>238</sup> U, <sup>232</sup> Th	Quartz	3.2 kg
SiPM Electronics	<sup>238</sup> U, <sup>232</sup> Th	ASICs	2.04 kg
SiPM Glue	<sup>238</sup> U, <sup>232</sup> Th, <sup>40</sup> K	Epoxy	0.12 kg
SiPM Cables	<sup>238</sup> U, <sup>232</sup> Th	Kapton	$1 \times 10^4$ cm <sup>2</sup>
Charge Module Cables	<sup>238</sup> U, <sup>232</sup> Th	Kapton	$1 \times 10^4$ cm <sup>2</sup>
Charge Module Electronics	<sup>238</sup> U, <sup>232</sup> Th	ASICs	1.0 kg
Charge Module Glue	<sup>238</sup> U, <sup>232</sup> Th, <sup>40</sup> K	Epoxy	0.35 kg
Charge Module Support	<sup>238</sup> U, <sup>232</sup> Th	Copper	11.7 kg
Charge Module Backing	<sup>238</sup> U, <sup>232</sup> Th	Quartz	0.94 kg
TPC LXe Volume	<sup>137</sup> Xe, <sup>222</sup> Rn, $2\nu\beta\beta$ , $0\nu\beta\beta$	Xenon	4038 kg
Outer LXe Volume	<sup>137</sup> Xe, <sup>222</sup> Rn, $2\nu\beta\beta$ , $0\nu\beta\beta$	Xenon	1071 kg

- Extensive radio-assay and background control program
- Comprehensive background modeling for sensitivity evaluation



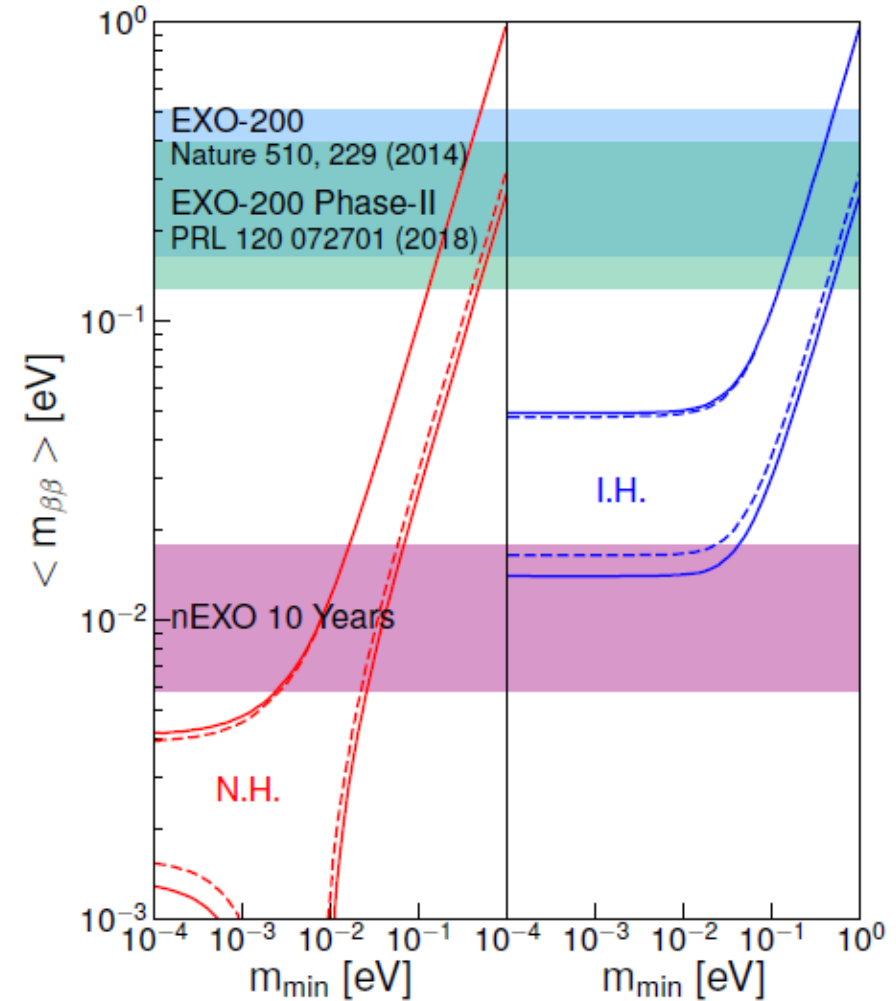
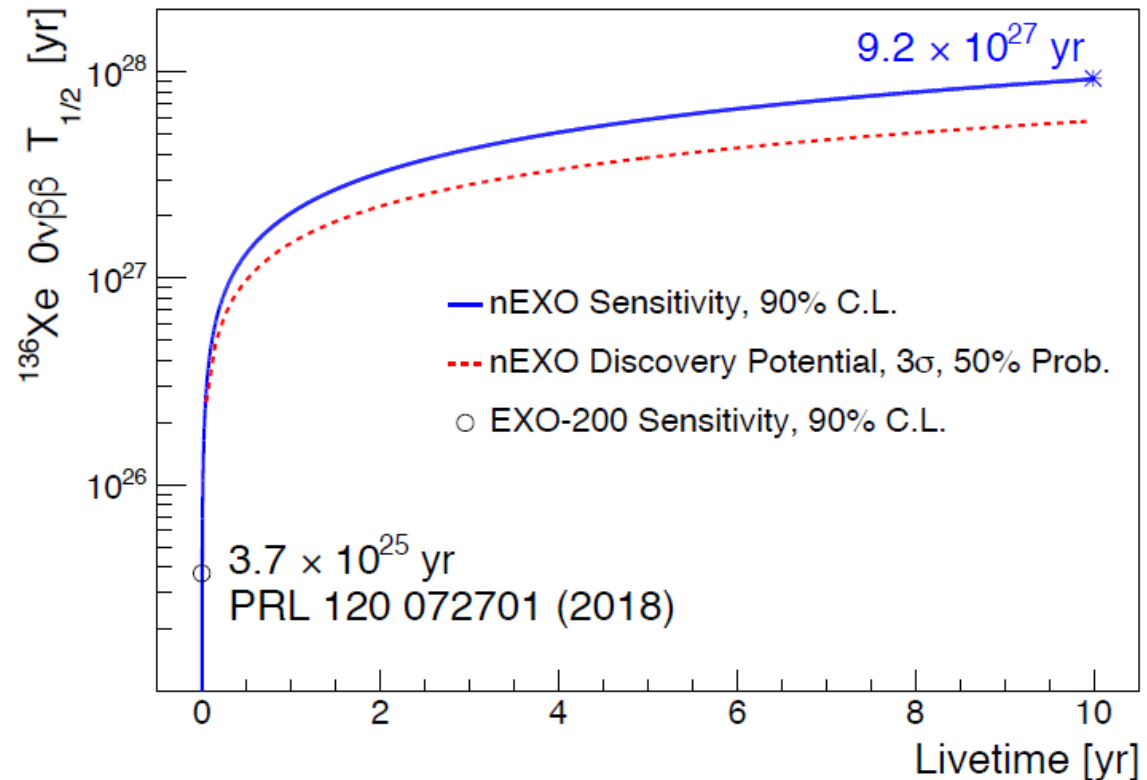
Assumed 0 $\nu\beta\beta$  half-life  
5.7e27 yr

# Multi-dimensional Fit vs Counting Experiment



Multi-variate analysis maximize the sensitivity to  $0\nu\beta\beta$  than simple counting experiment.

# Ultimate sensitivity



\* 20-30% additional improvement with machine learning  
discriminator *JINST* 14 (2019) 09, P09020

\* New sensitivity evaluation with improved radio-assay data,  
detector design and analysis will be released soon!

# nEXO publications (since 2018)

- **Reflectivity of VUV-sensitive Silicon Photomultipliers in Liquid Xenon**, M. Wagenpfeil, et al, arXiv:2104.07997 (2021)
- **Event Reconstruction in a Liquid Xenon Time Projection Chamber with an Optically-Open Field Cage**, T. Stiegler, et al (nEXO), NIMA 1000, 165239 (2021)
- **Reflectance of Silicon Photomultipliers at Vacuum Ultraviolet Wavelengths**, P. Lv, et al (nEXO) IEEE Trans. Nucl. Sci. 67, 2501 (2020)
- **Reflectivity and PDE of VUV4 Hamamatsu SiPMs in liquid xenon**, P. Nakarim, et al (nEXO), JINST 15, P01019 (2020)
- **Measurements of electron transport in liquid and gas Xenon using a laser-driven photocathode**, O. Njoya, et al., (nEXO), NIM A 972, 163965 (2020)
- **Characterization of the Hamamatsu VUV4 MPPCs for nEXO**, G. Gallina, et al. (nEXO), NIMA 940, 371 (2019)
- **Simulation of charge readout with segmented tiles in nEXO**, Z. Li, et al., (nEXO), JINST 14, P09020 (2019)
- **Study of Silicon Photomultiplier Performance in External Electric Fields**, X.L. Sun, et al., (nEXO), JINST 13, T09006 (2018) (arXiv:1807.03007) (nEXO Collaboration)
- **VUV-sensitive Silicon Photomultipliers for Xenon Scintillation Light Detection in nEXO**, IEEE Transactions on Nuclear Science 1 (2018) (arXiv:1806.02220)(nEXO Collaboration)
- **nEXO Pre-Conceptual Design Report**, arXiv:1805.11142v2 (nEXO Collaboration)
- **Characterization of an Ionization Readout Tile for nEXO**, JINST 13, P01006 (2018) (arXiv: arXiv:1710.05109v1)(nEXO Collaboration)
- **Sensitivity and Discovery Potential of nEXO to Neutrinoless Double Beta Decay**, Physical Review C 97, 065503 (2018) (arXiv: arXiv:1710.05075v1)(nEXO Collaboration)
- **Imaging individual Ba atoms in solid xenon for barium tagging in nEXO**, Nature 569, 203 (2019) (arXiv:1806.10694)(nEXO Collaboration)



Laurentian University  
Université Laurentienne

>150 scientists, 34 institutions in 8 countries on 4 continents

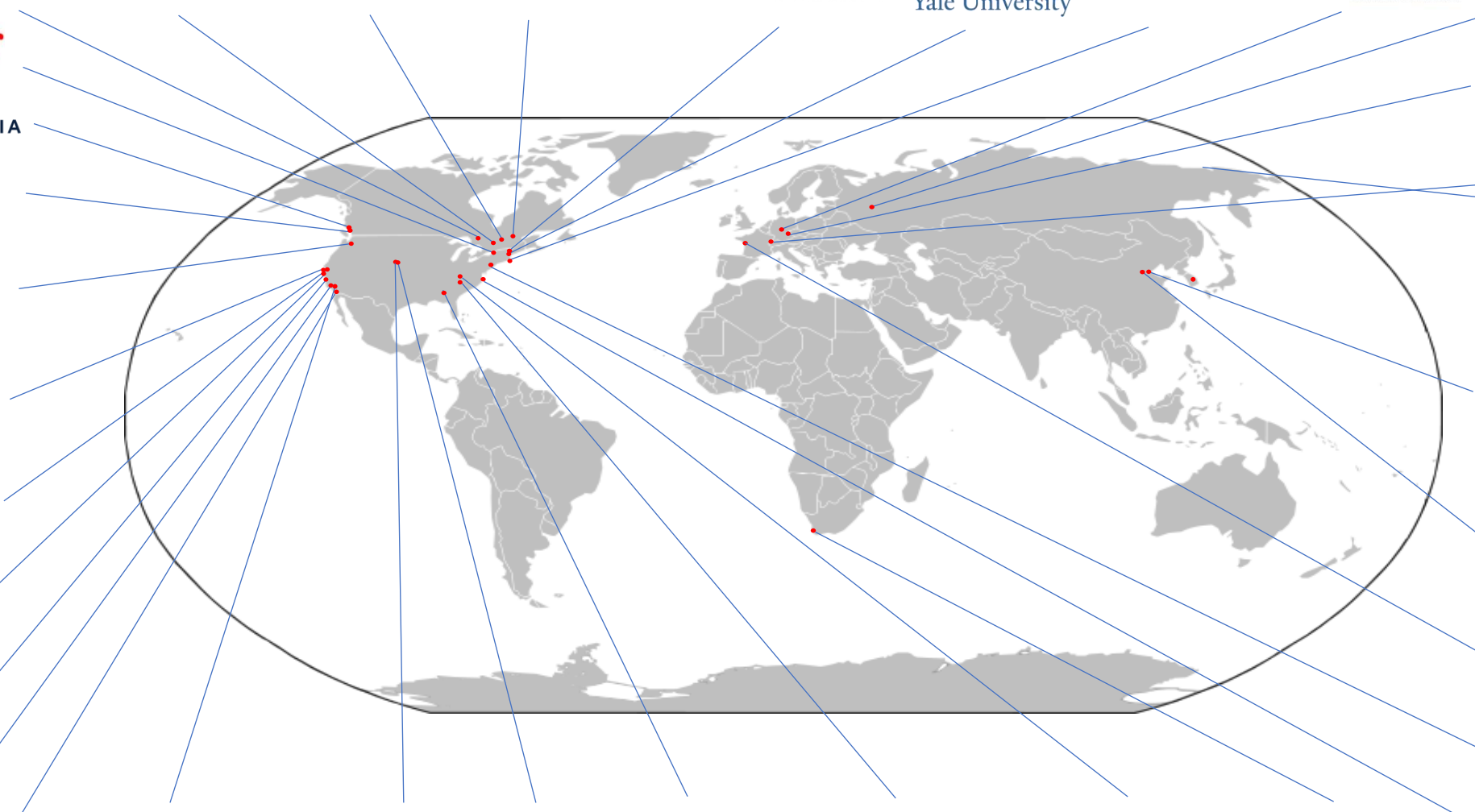


THE UNIVERSITY  
OF BRITISH COLUMBIA



Caltech

UC San Diego



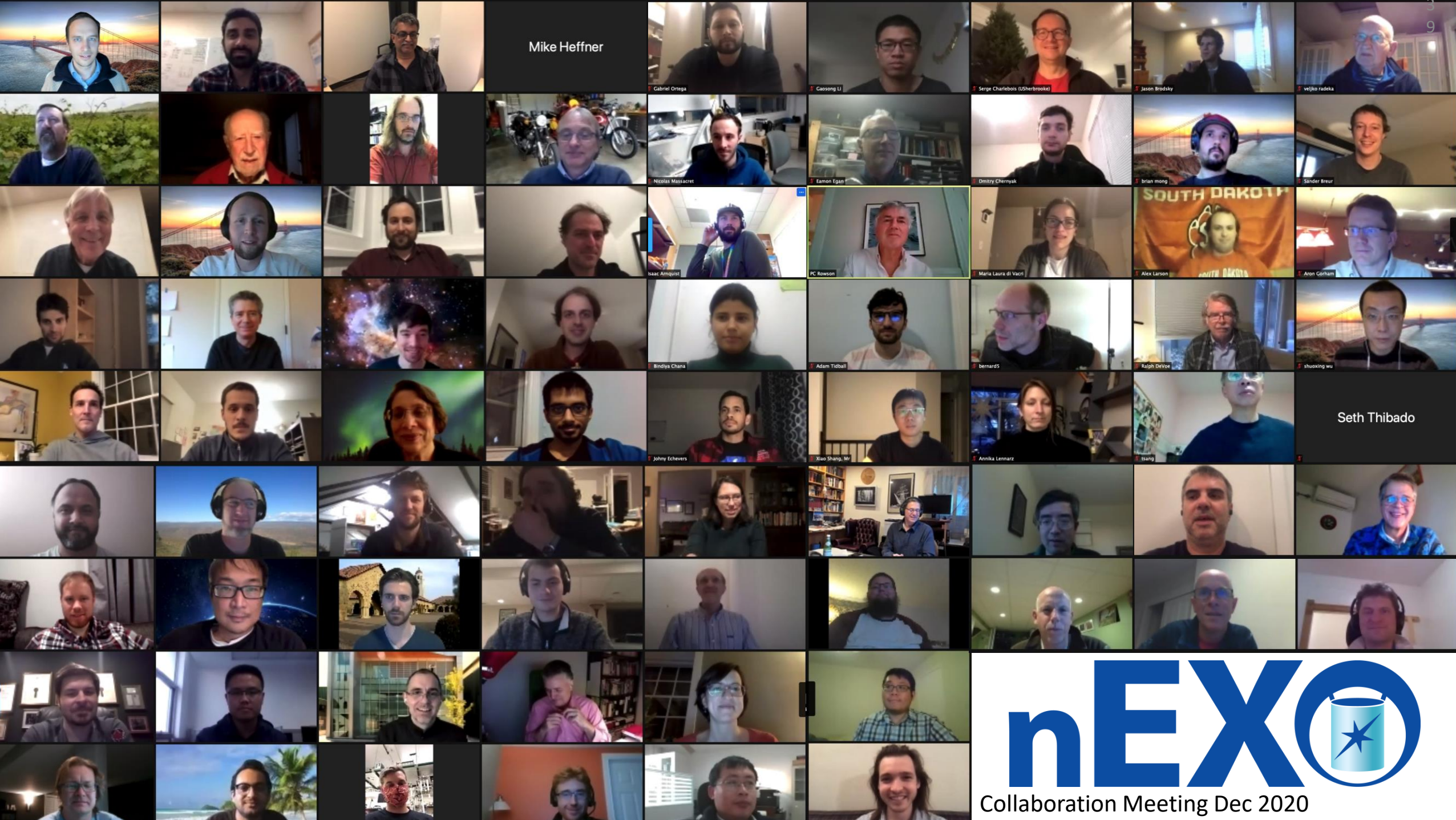
$u^b$

$^b$  UNIVERSITÄT  
BERN



UNIVERSITY of  
NORTH CAROLINA  
WILMINGTON

Mike Heffner



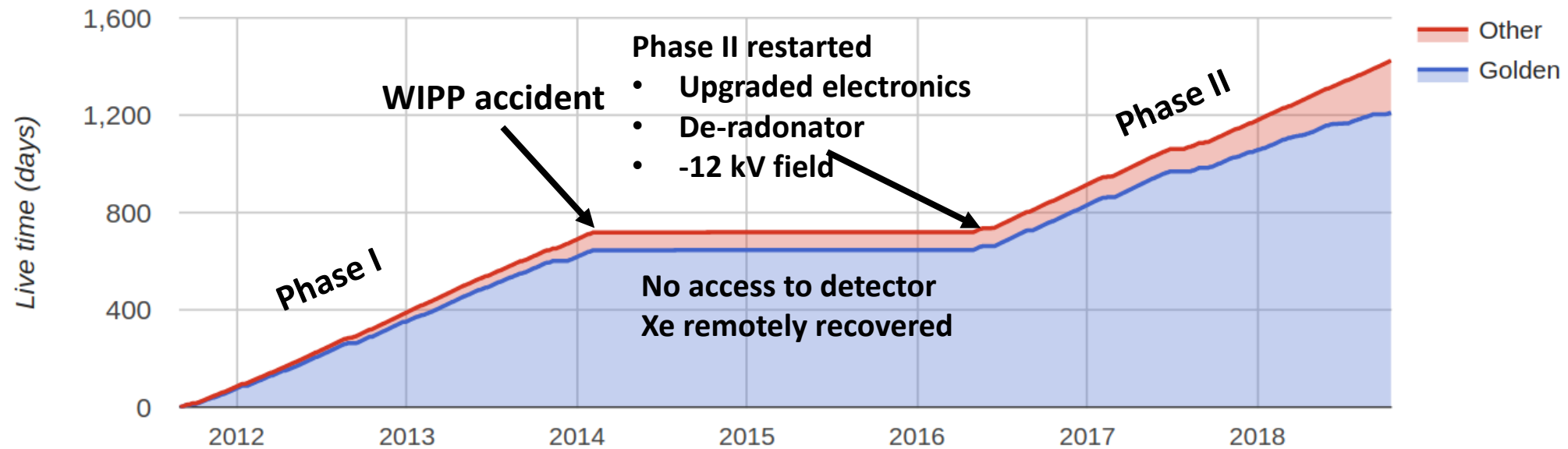
nEXO  
Collaboration Meeting Dec 2020

# Summary

- EXO-200 demonstrated the liquid xenon TPC technology for  $0\nu\beta\beta$  search
- nEXO is a discovery focused  $0\nu\beta\beta$  experiment, designed to reach a sensitivity beyond  $\sim 10^{28}$  years, based on extensive R&D work
- US DOE has scheduled a DBD portfolio review in July 2021
- Observation of  $0\nu\beta\beta$  always implies new physics!

# Backup

# EXO-200 timeline

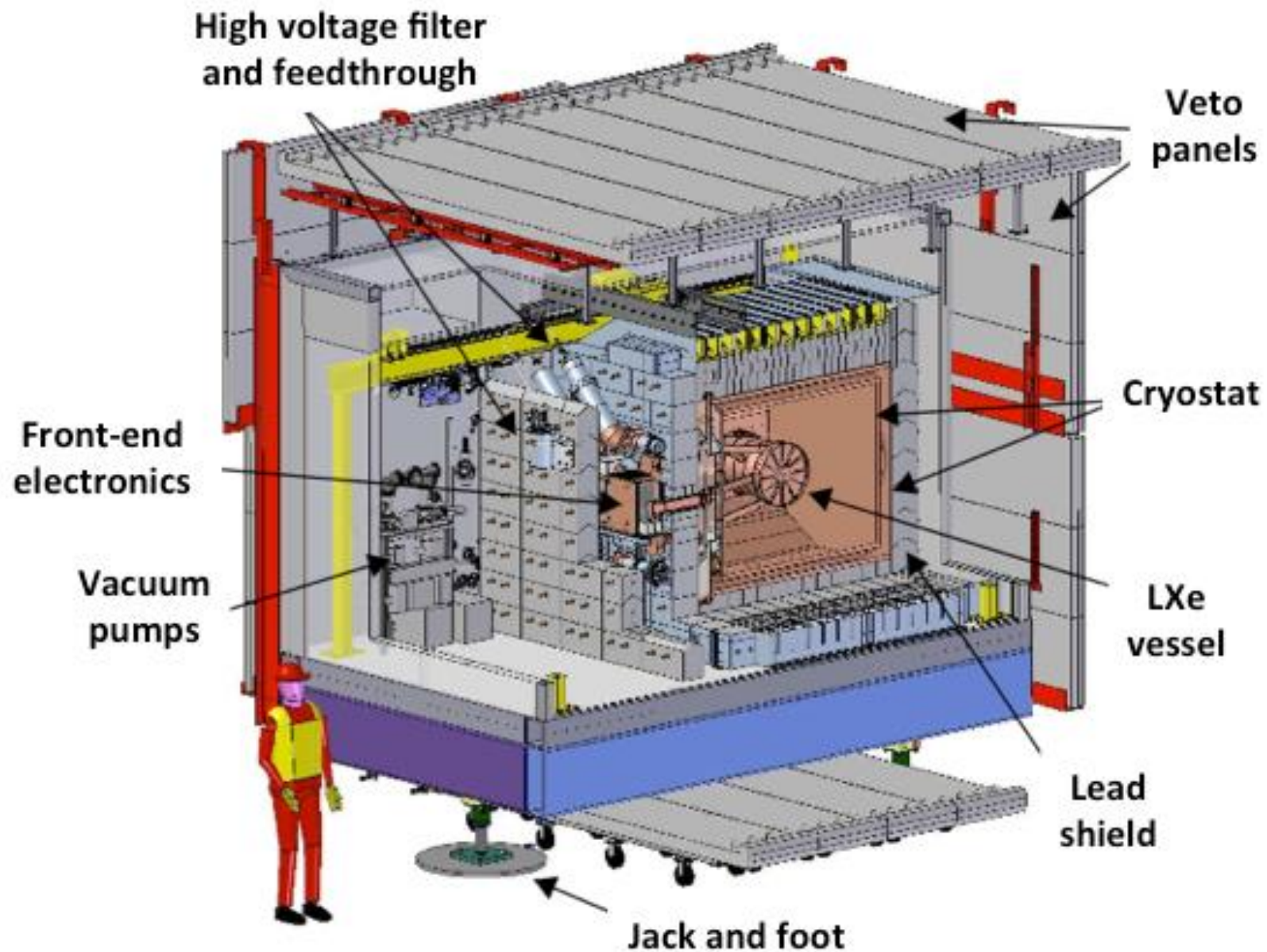


- Operation concluded in Dec 2018, with 1181.3 days of livetime
- Phase I from Sep 2011 to Feb 2014
  - Precise  $2\nu\beta\beta$  measurement, *Phys. Rev. C* **89**, 015502 (2013)
  - Stringent limit for  $0\nu\beta\beta$  search, *Nature* **510**, 229 (2014)
- Phase II operation begins on Jan 31, 2016 with system upgrades
  - First results with Phase II data from upgraded detector, *Phys. Rev. Lett.* **120**, 072701 (2018)
  - Final results with all exposure, *Phys. Rev. Lett.* **123** (2019) no.16, 161802

# EXO-200

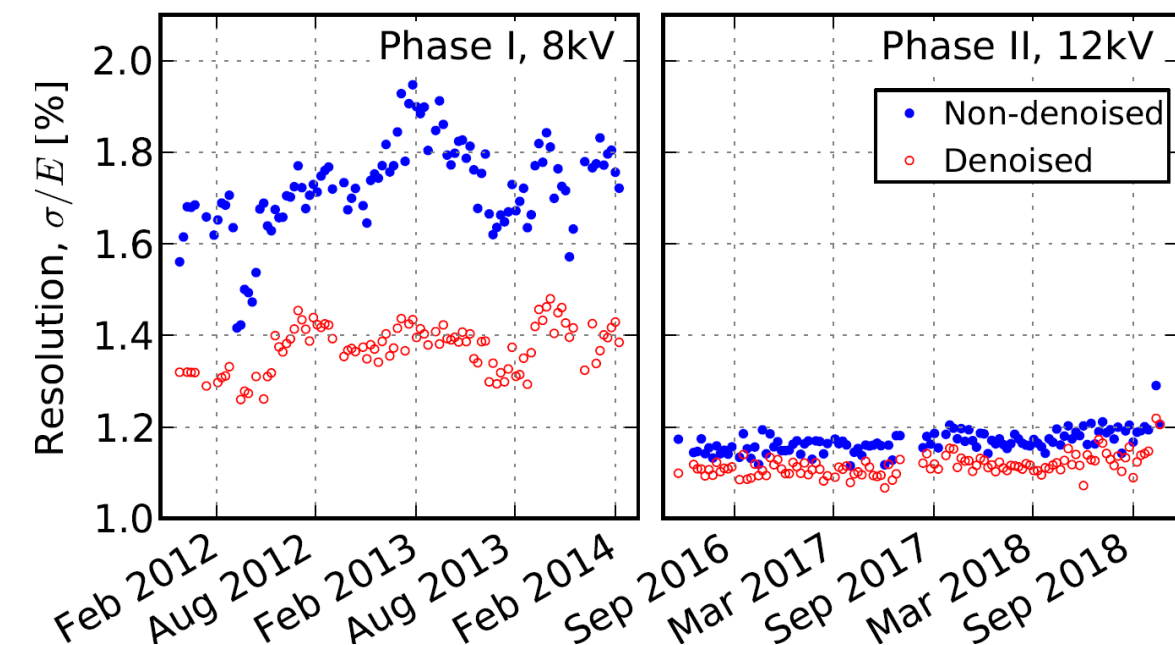
- Located at Waste Isolation Pilot Plant (WIPP) in Carlsbad, NM, USA
- 1624 m.w.e. overburden
- LXe vessel surrounded by ~50 cm HFE-7000 cryofluid, housed in a double-wall cryostat
- ~25 cm passive lead shield in all directions
- Plastic scintillator panels for muon veto

**Detector schematic:**



# Resolution improvement

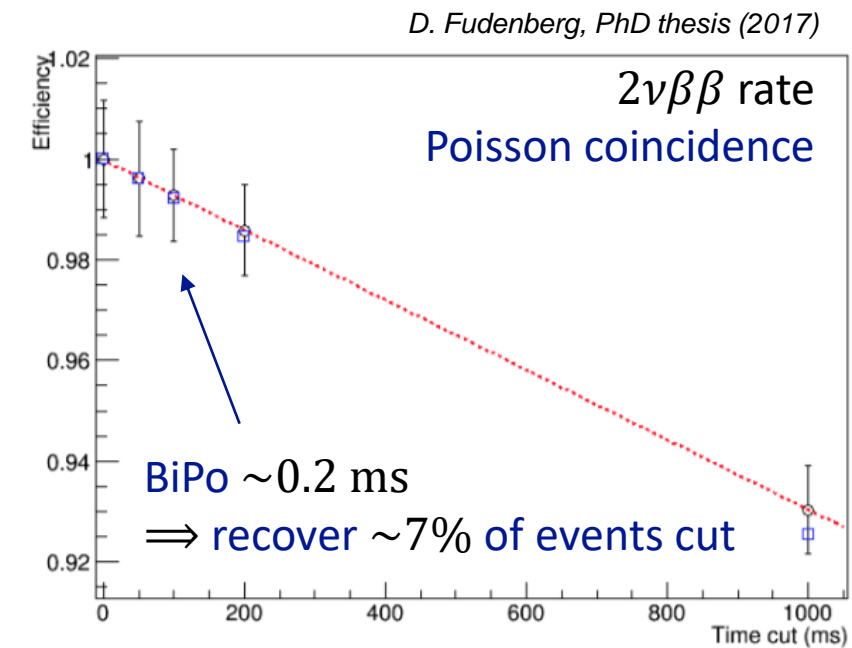
Resolution at the Q value ( $^{228}\text{Th}$  near cathode)



- Front end readout electronics
  - Reduce APD readout excess noise
- Cathode HV increased from -8 kV to -12 kV
- Software De-noising to optimize energy calibration
- **De-noising adapted for Phase II as well in new analysis**
- **Proper Modeling of mixed collection/induction wire signals**
- Energy resolution ( $\sigma/E$ ) at  $Q_{\beta\beta}$  value (design goal 1.6%)
  - Phase I:  $1.35 \pm 0.09\%$
  - Phase II:  $1.15 \pm 0.02\%$

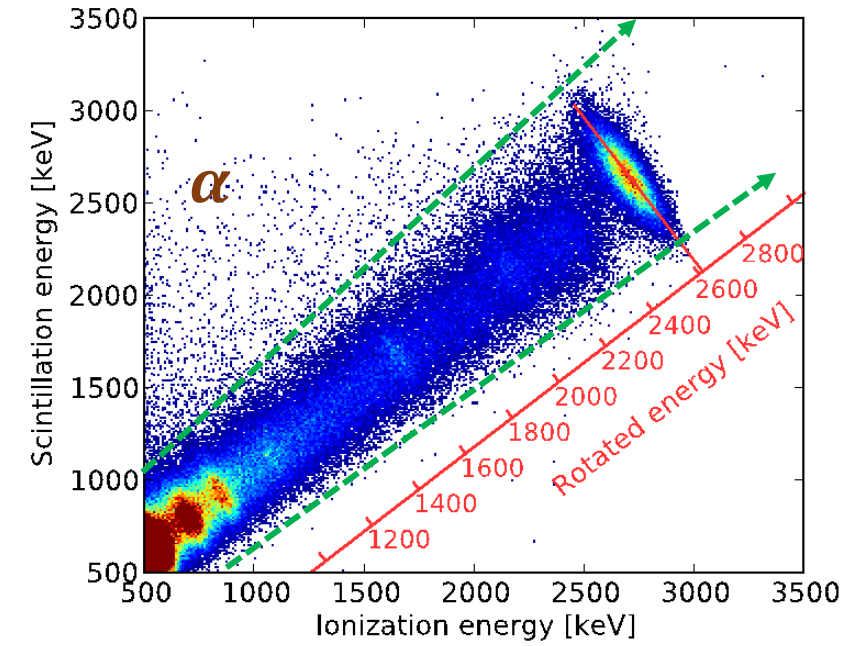
# Increasing $0\nu\beta\beta$ detection efficiency

- Another major signal efficiency loss in previous analyses has been improved in addition to the 3D cut
- Event coincidence cut
  - Originally designed to remove time-correlated events, e.g. Bi-Po event, potential muon induced long-lived decay products ...
  - Comprehensive cosmogenic background studies (*JCAP* 1604 (2016) no.04, 029) later found no evidence of contributions from such muon-induced isotopes
  - Reducing time cut window from 1s to 0.1 s is still sufficient for rejecting Bi-Po
- $0\nu\beta\beta$  detection efficiency increases from ~80% to  **$97.8 \pm 3.0\%$  ( $96.4 \pm 3.0\%$ ) for Phase I (II)**



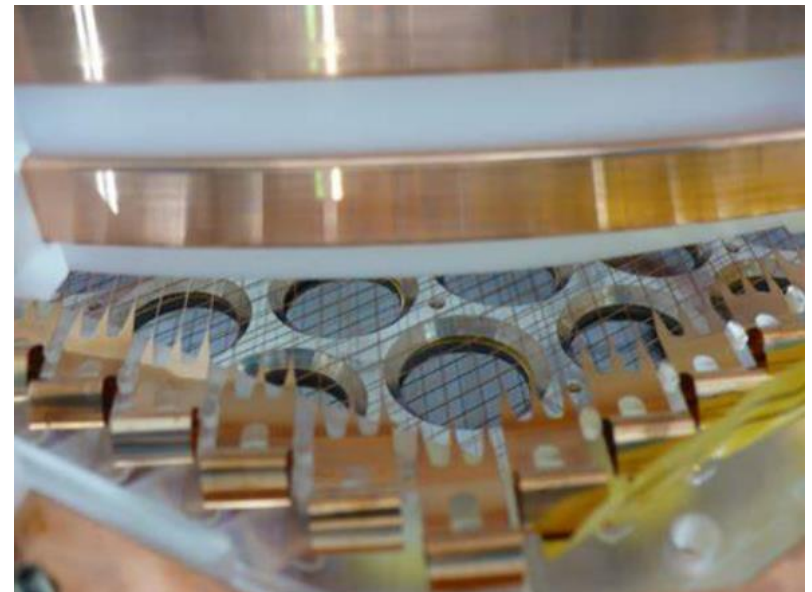
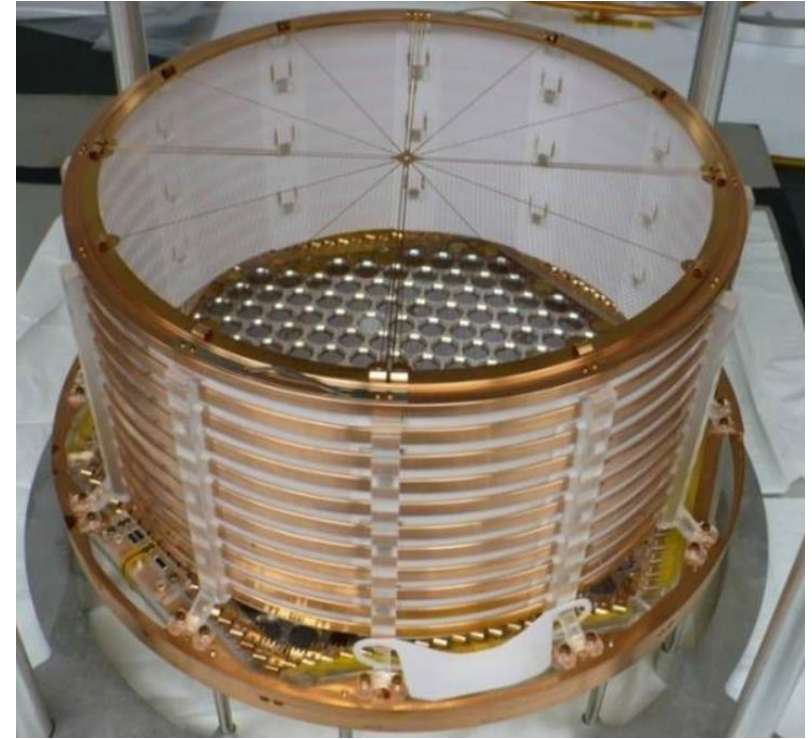
# Light/charge Diagonal cut

- Requires 2D light/charge energy calibration and good understanding of detector
- Light/charge ratio distributions validated by comparison between data/simulation using source and  $2\nu\beta\beta$  data
- Powerful to reject  $\alpha$ , as well as poorly reconstructed  $\beta/\gamma$  with anomalous light/charge ratio



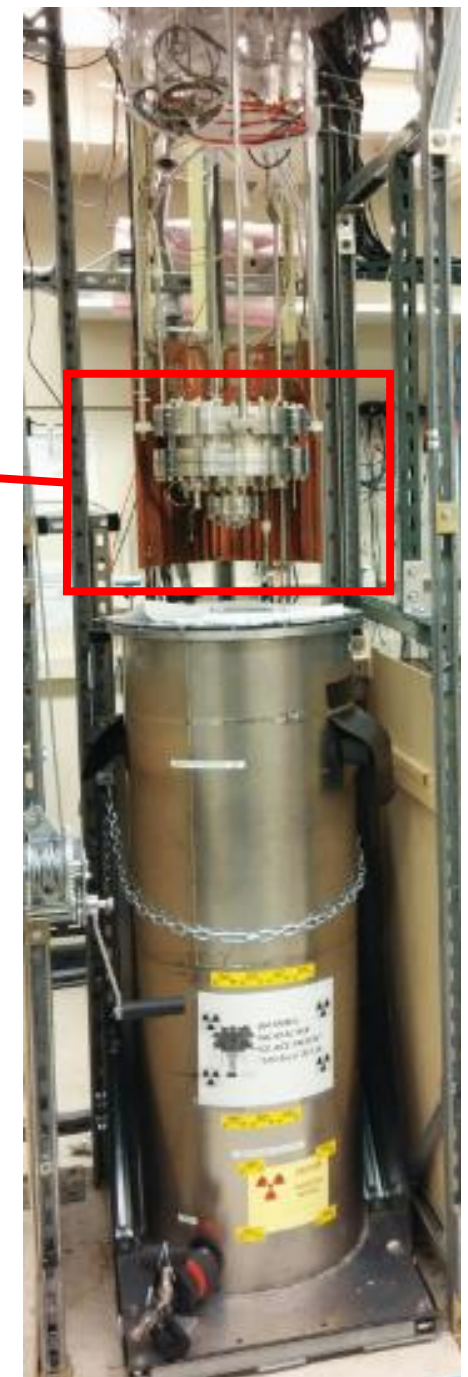
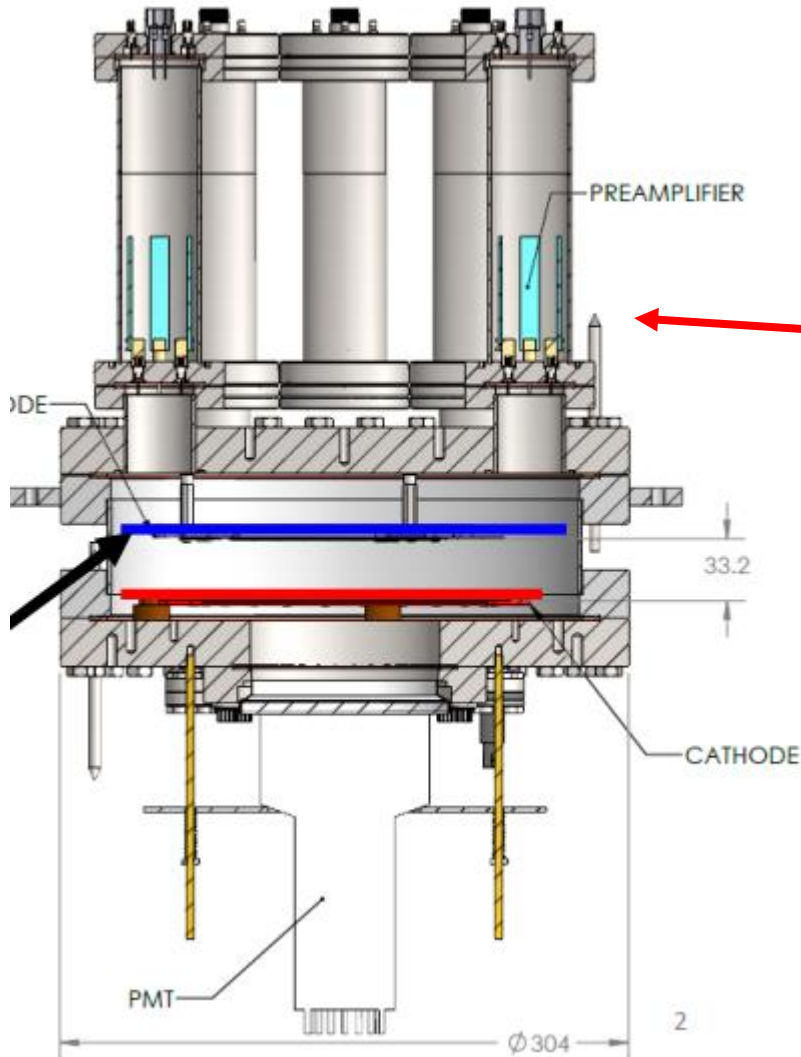
# Time Projection Chamber (TPC)

- Single phase liquid xenon TPC with  $^{enr}\text{Xe}$  (80.6%)
- $\sim 110$  kg active volume
- Two back-to-back TPCs with cathode in the middle
- Scintillation light readout by APDs
- Ionization charge detected by two wire grids crossing at 60 degree
  - Collection plane (U-plane)
  - Induction (shielding) plane (V-plane)



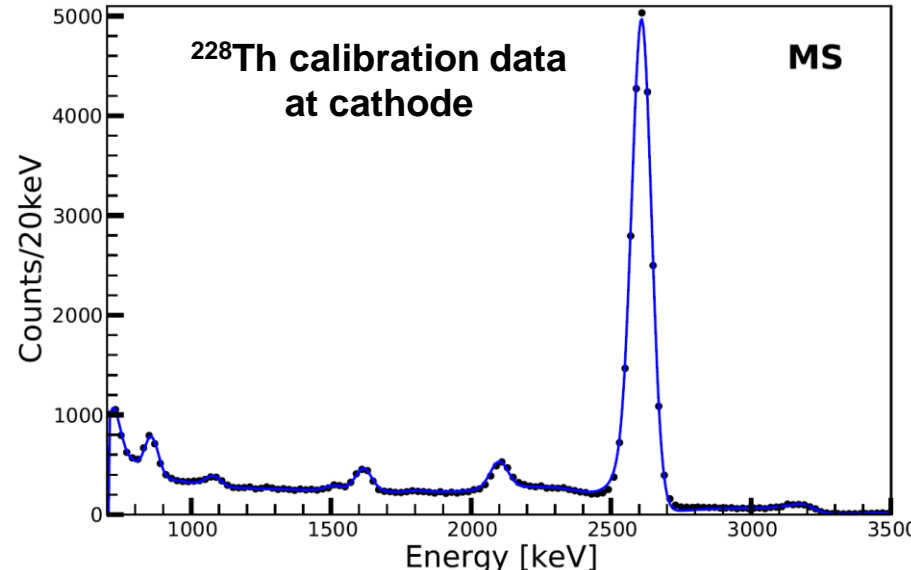
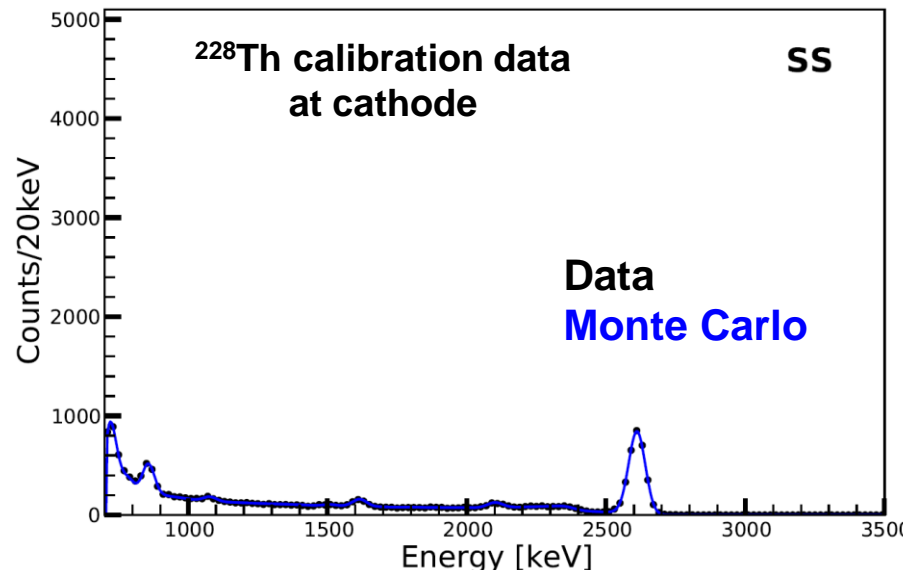
# Test stand TPC

- **3.3 cm drift length**
  - Operating at up to 1 kV/cm field
- Charge tile anode with
  - 30 X strips + 30 Y strips
- PMT for light detection
  - Low efficiency though
  - Used only for trigger

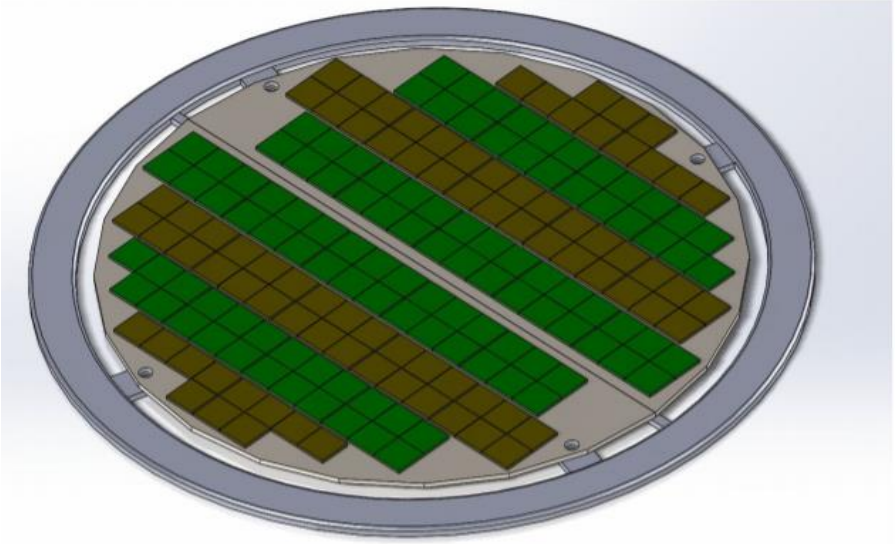


# Relaxed 3D cut

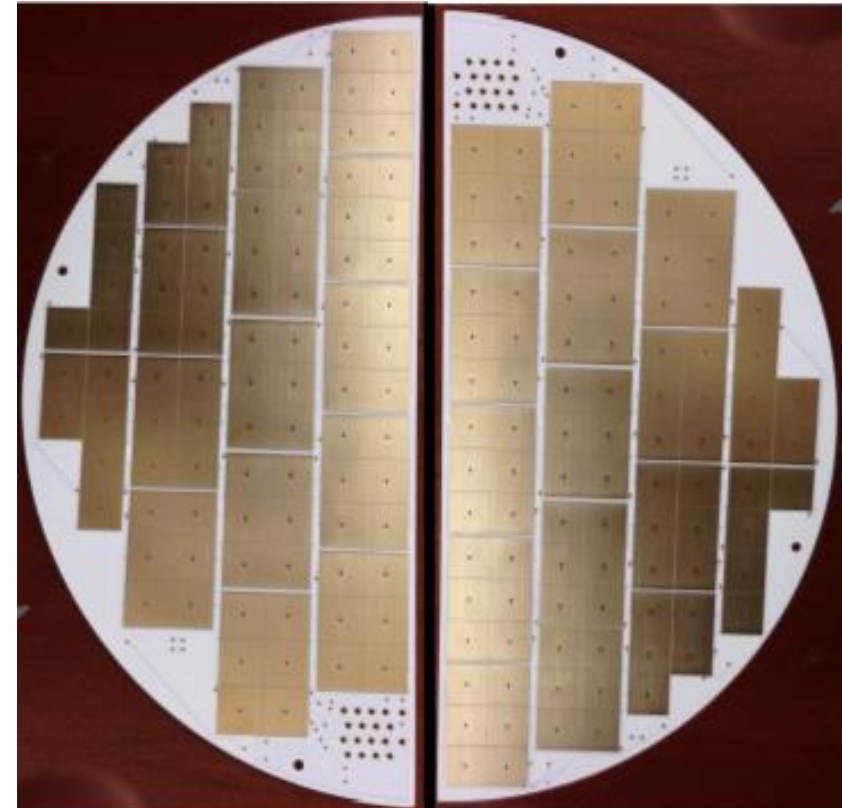
- Previous analyses require all events having full 3D position
- Partial 3D events are due to small energy deposit having complete collection on U-wire, but usually having no V signals because of higher threshold
- Now require >60% of energy deposits having 3D position, only recovering MS events
- Recovers almost all previously cut  $0\nu\beta\beta$  events (10%) in MS due to small bremsstrahlung deposit
- Average SS fraction is **12%** in the energy range  $Q_{\beta\beta} \pm 2\sigma$  for Th-228 source deployed near the cathode



# large area SiPM array Integration R&D



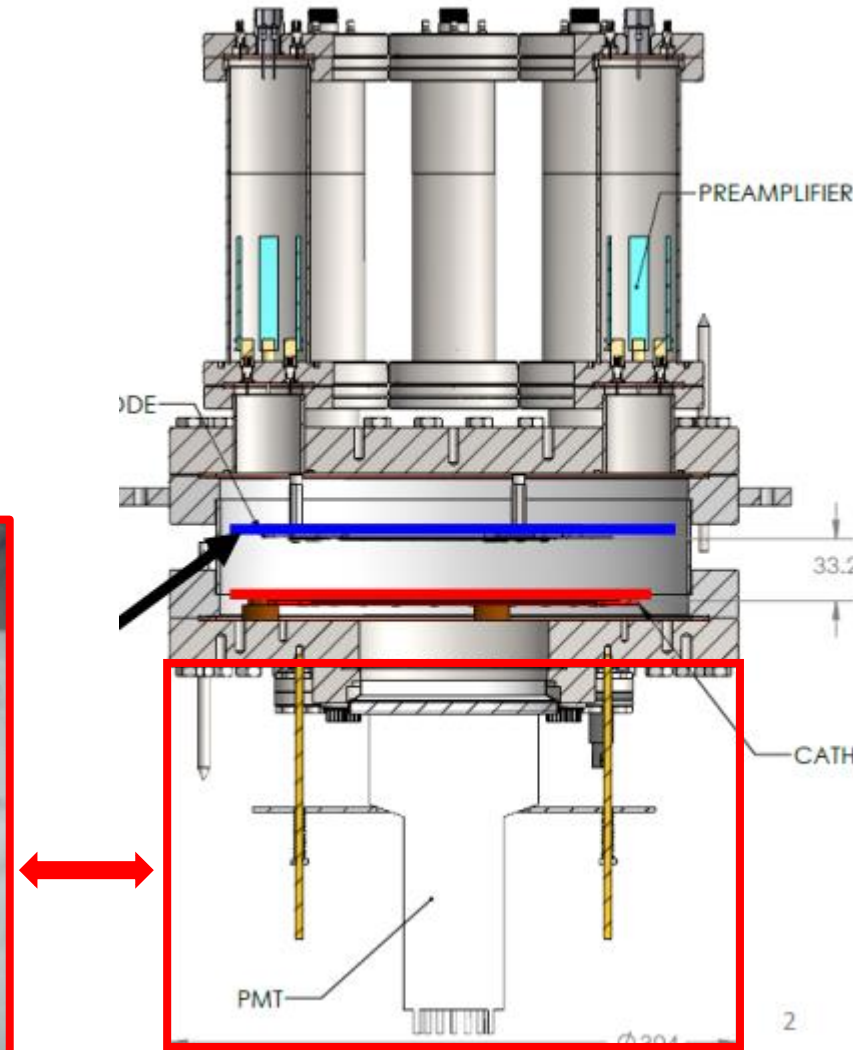
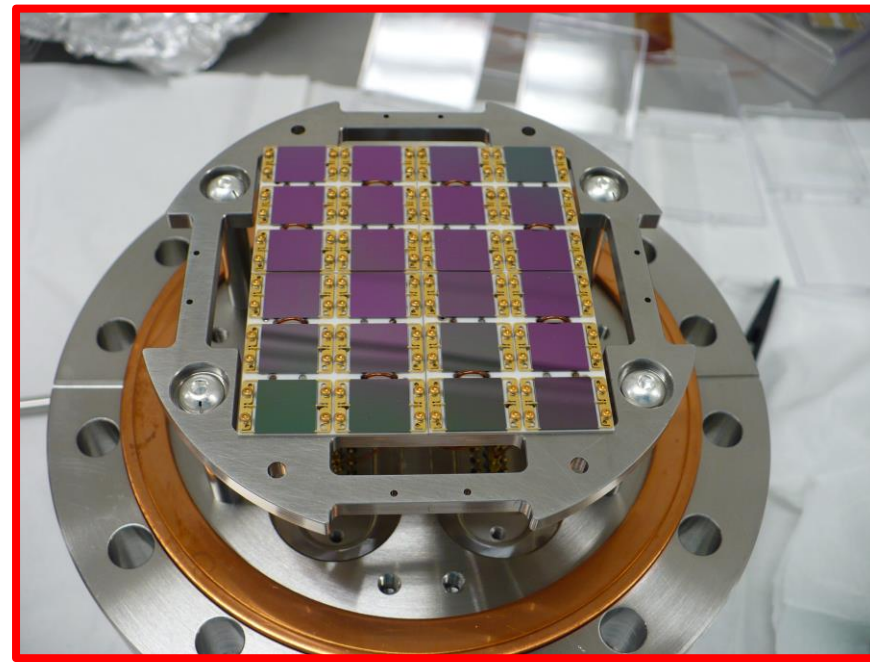
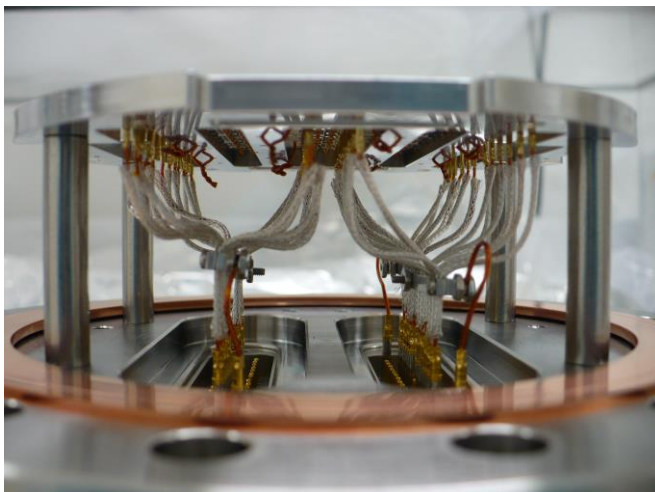
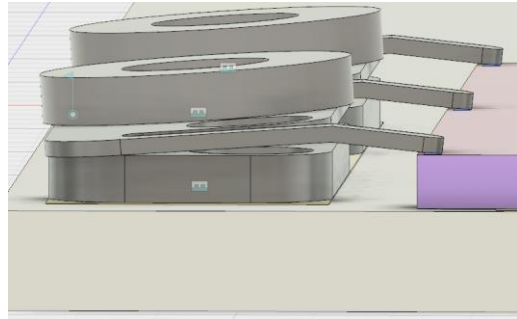
- A larger array with ~200 devices is being build
- New design optimized for **light collection efficiency**
- x10 increase in number of channels give rise to new technical difficulties
  - Individual DC bias for each channel with constraints in board size and low temperature
- Important to demonstrate 1% energy resolution goal with the nEXO-style charge-tile and SiPM readout
- Important R&D demonstration for DOE down selection!

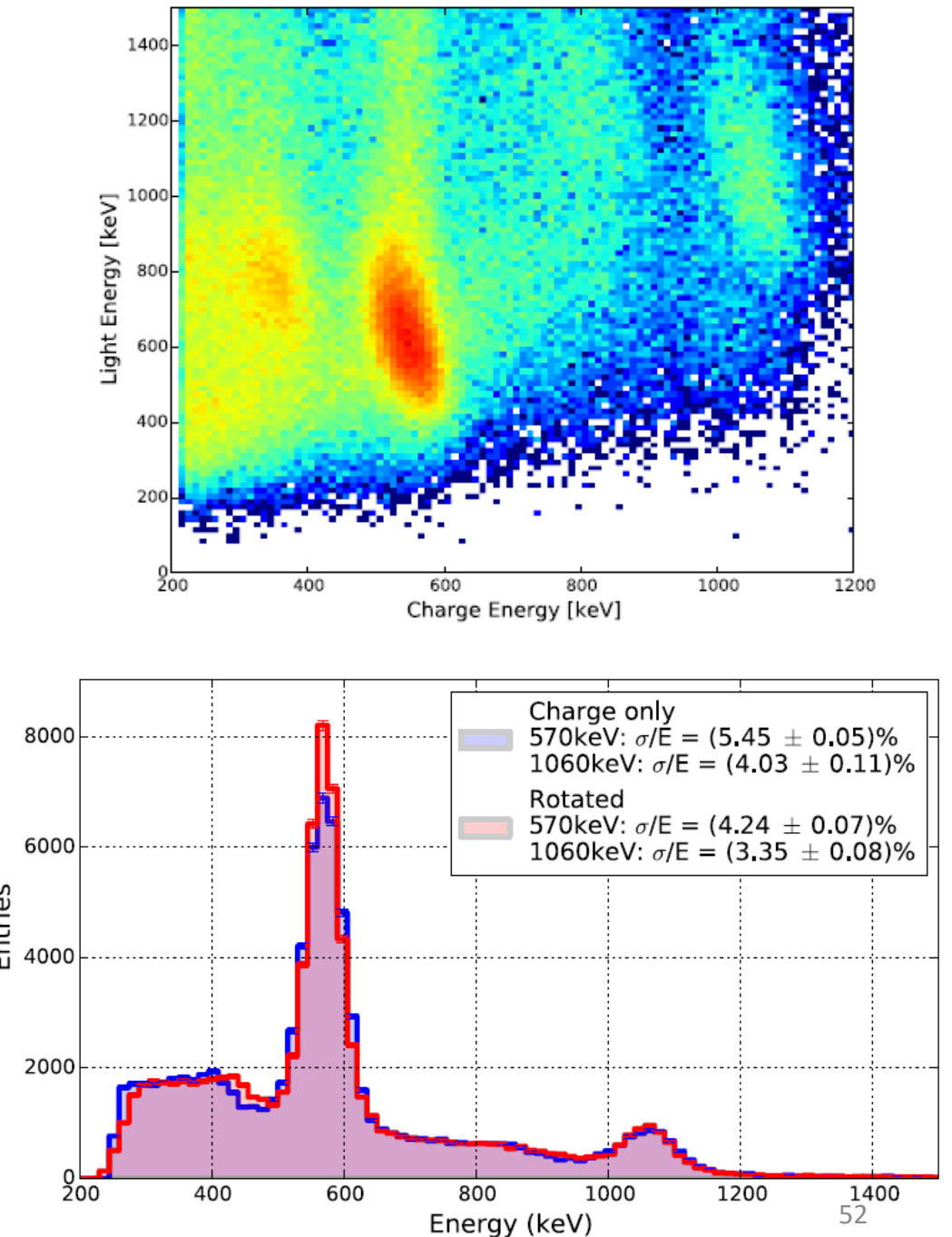
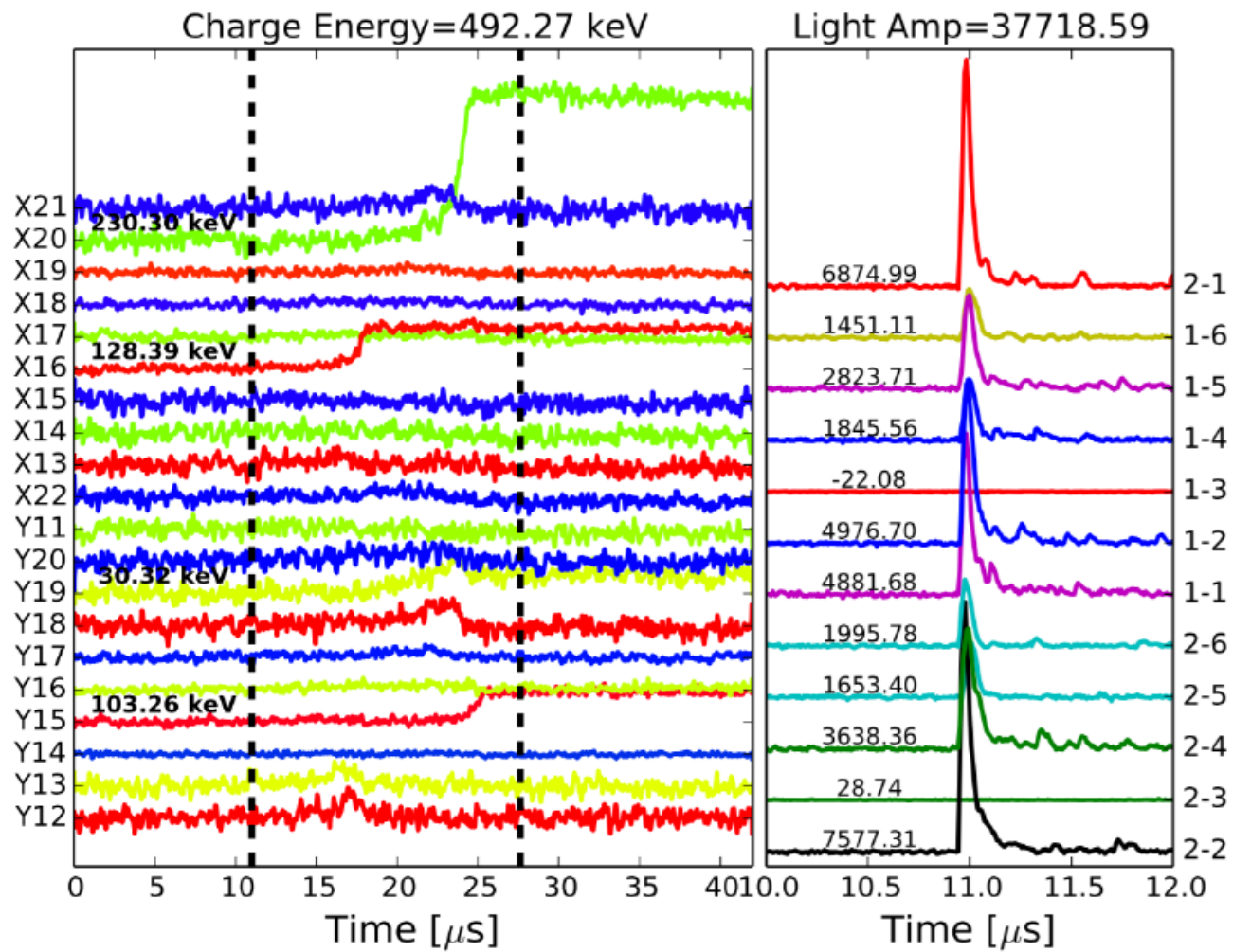


Ceramic carrier 50

# Integrate large area SiPM array to the test stand

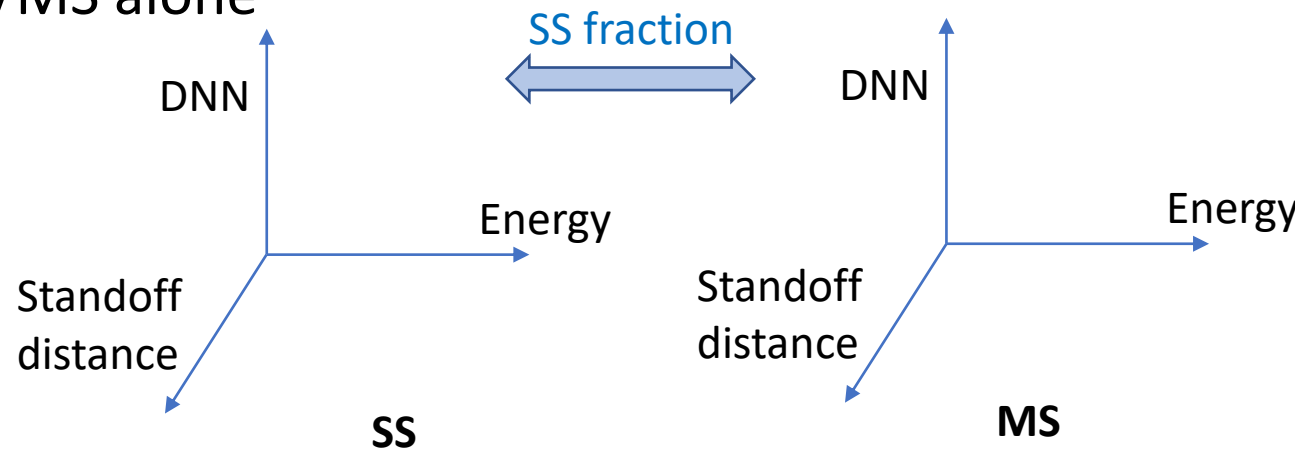
- Implemented an array of 24 SiPMs ( $24 \text{ cm}^2$ ) to replace the PMT in the test stand for light detection
  - The first close-to-nEXO-style detector
  - Improved light collection efficiency (5-10x)

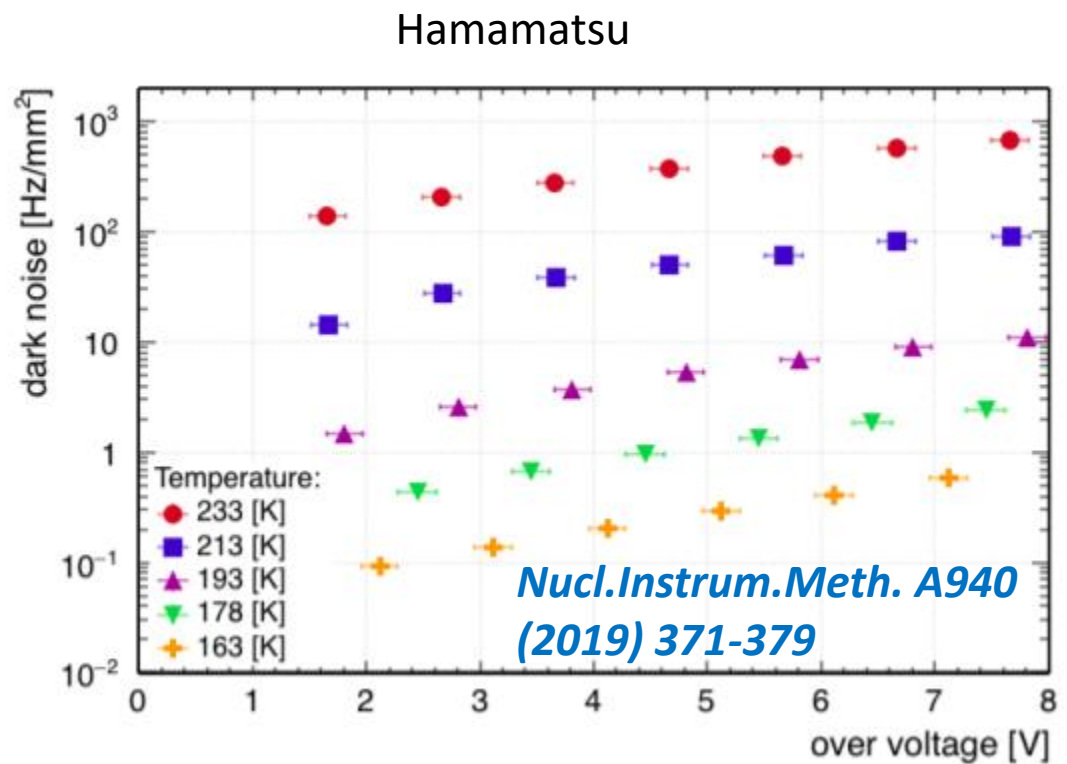
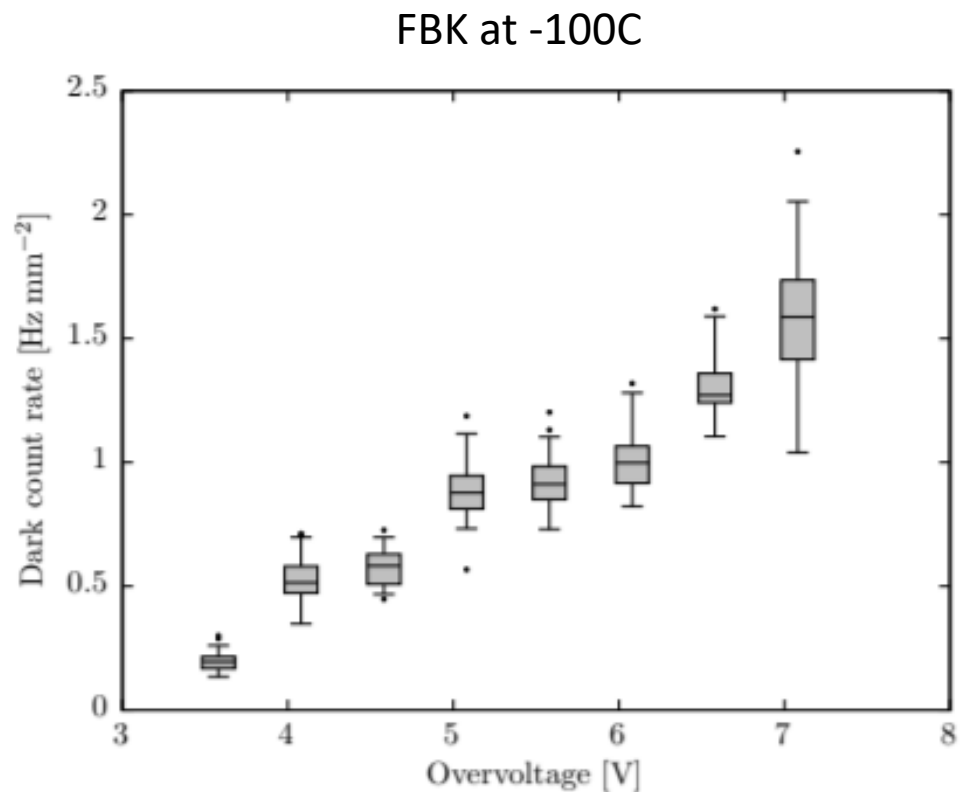




# Analysis strategy

- Blinded analysis performed
- SS/MS classification
- 3-dimension fit in both SS and MS: **E + DNN + standoff distance**
  - Energy, event topology and spatial information
  - Make the most use of multi-parameters for background rejection
  - SS, MS relative contributions constrained by SS fraction
- Improvement of **~25%** in  $0\nu\beta\beta$  half-life sensitivity compared with using energy spectra + SS/MS alone





- At 4V operation voltage and LXe temperature, dark count rate < 1Hz/mm<sup>2</sup>
- Hamamatsu is better than FBK, achieves ~0.2 Hz/mm<sup>2</sup>